Center for Advanced Materials

CAM

Dopant Effects on Sintering Behavior in Ceramic Matrix Composites

G.L. Brown
(M.S. Thesis)

December 1990

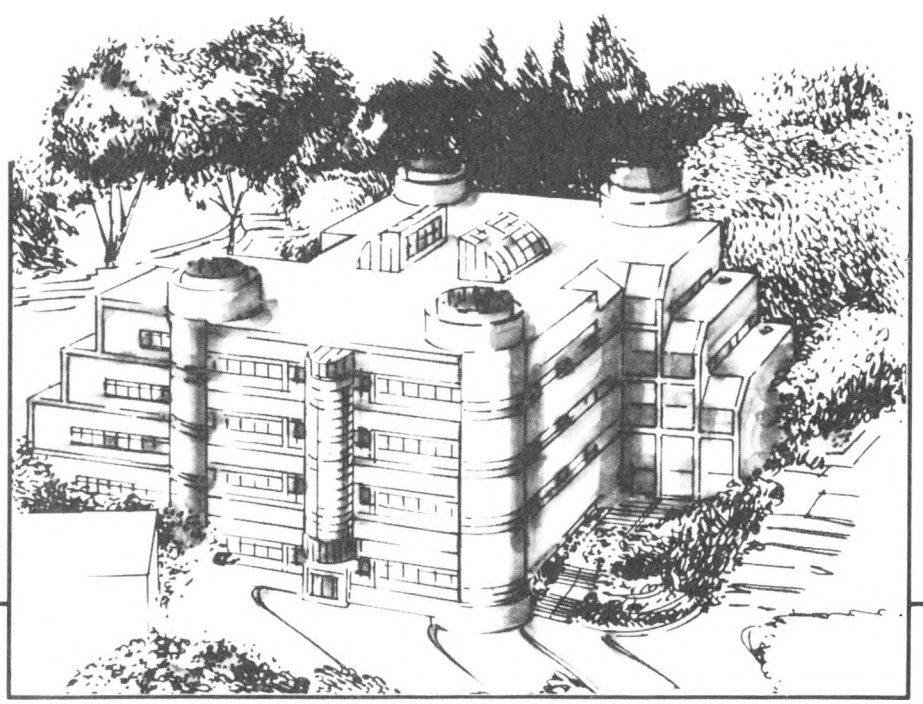

Materials and Chemical Sciences Division

Lawrence Berkeley Laboratory • University of California

ONE CYCLOTRON ROAD, BERKELEY, CA 94720 • (415) 486-4755

Prepared for the U.S. Department of Energy under Contract DE-AC03-76SF00098

LBL--30220

DE91 009774

Dopant Effects on Sintering Behavior in Ceramic Matrix Composites

Gillian L. Brown
(M.S. Thesis)

Department of Materials Science and Mineral Engineering,
University of California

and

Materials and Chemical Sciences Division,
Lawrence Berkeley Laboratory
University of California
Berkeley, California 94720

December, 1990

This work was supported by the Division of Materials Science, Office of Basic Energy Research, United States Department of Energy, Under Contract No. DE-AC03-76SF00098 with the Lawrence Berkeley Laboratory.

ACKNOWLEDGEMENTS

Many thanks to Professor Lutgard C. De Jonghe for his guidance and helpful advice during this work. I am also grateful to my co-workers, for their suggestions and support. In particular, I would like to thank Max Ghirlanda for sharing his knowledge of sintering theory during many useful discussions, and Thea Buchanan for her help with general ceramics processing techniques. Finally, thanks to my family in Jamaica without whose support and encouragement throughout my education, this work could not have been completed.

Table of Contents

1. INTRODUCTION

Heterogeneities present one of the most serious problems in the processing of ceramic bodies. Non-uniformities in a ceramic, such as agglomerates, rigid inclusions, a wide particle size or pore size distribution, or spatial variations in green density can seriously affect sintering behavior, and experiments performed on highly uniform powder compacts have proven the importance of homogeneity within the compact [1-3]. Powder compacts produced by conventional processing techniques, however, usually contain at least some of the inhomogeneities mentioned above. Not only do these inhomogeneities retard densification, but they also cause microscopic damage, such as the formation of crack-like flaws or large pores around inhomogeneities [4], which are detrimental to the mechanical properties of the sintered body.

Particulate ceramic composites are currently being studied a great deal because of their improved fracture toughness and high-temperature creep resistance over single-phase ceramics. The presence of an inert second phase, however, has been found to hinder the densification of the matrix material seriously , even at low volume fractions of the inclusion phase [5-7], in a way that is to date not fully understood. Such techniques as hot pressing, hot isostatic pressing, or the incorporation of liquid-phase forming additives must therefore be used to obtain theoretical or near-theoretical densities; however it would be more convenient and more economical to free sinter these composites to full density. It is therefore important to obtain an understanding of the exact effects of heterogeneities on sintering, so that these effects may be countered. In this study, an attempt was made to more fully understand the effects of rigid, non-sinterable inclusions on densification in the ZnO-SiC system.

1.1 BACKGROUND

Many scientists have attempted, over the past five to ten years, to explain the observed reduction in densification rate when rigid inclusions are added to a polycrystalline ceramic matrix. In general, all explanations start from a basic sintering model in which the driving force for sintering is considered in terms of a "sintering potential" [8], a "sintering pressure" [6], or a "sintering stress" [9]. This driving force is due to the tendency of a compact to reduce its free energy by replacing solid-vapor interfaces (pore surfaces) with solid-solid interfaces (grain boundaries), and by decreasing the number of solid-solid interfaces by grain growth. In the work of DeJonghe et al. [9], for example, the driving force is considered in terms of an equivalent, externally applied stress, which would produce the same densification rate as the compact's internal surface tensions. This "sintering stress", Σ, is related to the densification rate, $\dot{\varepsilon}_d$, by the following equation:

$$\Sigma = \eta_d \dot{\varepsilon}_d \tag{1}$$

where η_d, called the densification viscosity is a single term encompassing all kinetic and geometrical parameters, roughly given by [10]:

$$\eta_d = A \frac{kTG^3}{3D_b \delta_b} \tag{2}$$

for grain boundary diffusion, described by Coble. Here, A is a constant, G is the grain size, D_b is the grain-boundary diffusion coefficient, and δ_b is the grain boundary thickness.

Inhomogeneities are known to induce differential densification rates, and therefore the generation of stresses in the matrix material, which oppose the sintering stress [11]. These transient, and sometimes residual stresses, unless relieved by local shearing, or creep, will reduce the achievable endpoint density, and may cause structural damage [4, 8]. Creep behavior may be described by an equation analogous to that for densification:

$$\sigma_c = \eta_c \dot{\varepsilon}_c \tag{3}$$

where σ_C is the stress which causes shear deformation, η_C is the creep viscosity, given by:

$$\eta_c = A' \frac{kTG^3}{3D_b \delta_b} \tag{4}$$

and $\dot{\varepsilon}_c$ is the creep rate. The creep processes which arise due to the presence of these stresses have been investigated by various researchers; in particular, the technique of loading dilatometry has been developed by DeJonghe et al. [12], in which small uniaxial stresses may be applied to a sintering compact, in order that densification and creep behavior may be simultaneously monitored. This has proven a valuable technique for two reasons. First, the ratio of $\dot{\varepsilon}_d : \dot{\varepsilon}_c$ can be used to ascertain the sintering stress [13, 14]. Second, the contribution of creep processes to the densification of composites can be investigated.

In all models, then, the resistance to densification caused by the presence of rigid inclusions may be regarded as being due to a hydrostatic backstress, generated in the matrix, which opposes the driving force for sintering. At this point, however, the

explanations diverge, as the origin of the backstress is attributed to different phenomena, as reviewed below.

1.1.1. VISCOELASTIC BACKSTRESSES

Certain authors proposed [15,16] that the mismatch in shrinkage between the densifying matrix material and rigid, non-sinterable inclusions causes an appreciable tensile stress to develop in the matrix. Starting from the general force balance:

$$\bar{\sigma_m}(1-f) + \bar{\sigma_p} f = 0 \tag{5}$$

where $\bar{\sigma}$ = mean stress,

m, p, denote matrix and particle, respectively,

f = volume fraction of inclusions,

and since deviatoric creep should always occur to relieve the backstresses, they derived the equivalent, time-dependent viscoelastic stresses [15], using Laplace transforms, given by

$$\sigma_m(t) = \int_0^t -4G_m f \dot{\varepsilon_m} exp\{-G_m(t-u)/\eta_m\} du \tag{6}$$

where G_m = the matrix shear modulus,

and u = dummy variable.

Later, however, DeJonghe et al [9] showed that the backstresses generated relax relatively rapidly, when compared with the rate at which they are generated, thus rendering the viscoelastic treatment unnecessary. Furthermore, Scherer [17] proved that the stresses

predicted by this model (60 to 90% of the sintering stress) cannot accurately represent the magnitude of the actual backstress generated in the matrix, unless the Poisson's ratio of the matrix material is negative.

Scherer further suggested that the variation in the densification rate with volume fraction of inclusions could be described by a simple rule of mixtures (where the densification rate of the inclusions is zero), coupled with the backstress generated by the inclusions. This theory has been shown to hold true for the sintering of glass matrix composites (which undergo viscous sintering) at low volume fractions of inclusions ($f \leq 0.15$), but not at higher volume fractions, where the stress fields due to the inclusions overlap [18]. The model does not hold for composites of polycrystalline matrices, from which it may be inferred that these composites do not sinter by viscous mechanisms [19].

1.1.2. CONSTRAINED NETWORK MODEL

In this model, proposed by Lange [20] and later revised [21], composites are modeled as powder mixtures in which rigid inclusions are located at the nodes of a regular lattice network, where each inclusion is shared by four unit cells. When the composite shrinks, the network also shrinks (undergoing the same strain) without changing its shape. Strain compatibility should require that each unit cell retain its shape during densification, thereby imposing a constraint on the shrinkage of its neighbors. Lange argued that, since there is more powder between inclusion pairs located along unit cell diagonals than there is between adjacent inclusions along cell edges, and since the shrinkage between all sets of inclusion pairs should be the same for shape retention, powder along unit cell edges will attain a higher matrix density than that along diagonals. The powder along cell diagonals is

therefore constrained from shrinking to the same density as the powder along cell edges by the uniformly shrinking network of inclusions. It was therefore suggested that, in a composite containing a random distribution of inclusions, regions in which inclusions are closer together than average would reach a higher density than, and constrain those in which the inclusions are farther apart. Hence, unless extensive shear deformation of the network occurs, or the regions of lower density are able to deform the higher density regions to relieve the constraint, the matrix material will not densify fully.

In experiments on the Al_2O_3-ZrO_2 system [22], Lange et al. found that there are indeed networks of dense material surrounding regions of low density, and concluded that the network strain is the same as that of the composite, although he was not able to prove that the denser regions were associated with higher inclusion contents. He further observed that, in dense regions, grain growth occurred, while in regions of lower density, previously sintered grains separated to produce very large voids. He suggested that during sintering, the denser, larger-grained region will have a diminished capacity for the shear (creep) processes necessary for the densification of the less dense region, and that the sintering stress of the lower density regions will be consumed, and the free energy lowered during a "desintering" process. During "desintering", there is a break in the necks during grain coarsening and void coalescence.

This theory was also used to explain why the sintering of glass powders is less affected by the presence of rigid inclusions, as glass powders do not develop grain boundaries, and would therefore not desinter, and since glass powders would not experience the reduction in creep rate caused by grain growth. However, convincing experimental evidence is still required that such a model can explain the drastic reduction in

densification rate observed at as low as 3 vol% [5] of inclusions, as DeJonghe and Rahaman have shown that the expected opposition to densification caused by a heterogeneous distribution of inclusions is only significant at relatively high volume fractions (> 10 vol%).

1.1.3 PROCESSING-INDUCED DEFECTS

In one set of experiments by Lange [23], it was found that 80% of samples which had been slip-cast around dense cylindrical cores, developed microcracks during drying and heating. The cracks were initiated at agglomerates, and grew during subsequent sintering. In specimens in which no cracks were initiated, sintering to high densities without accompanying sintering damage was possible. Lange concluded that a single rigid inclusion cannot constrain the densification of the surrounding matrix material, that the origin of the hydrostatic backstress is in the differential strains developed during fabrication of the green body, and that these differential strains eventually cause sintering damage. He also proposed that a green body is most prone to damage in the period before neck formation. Later, it was also proposed by DeJonghe and Rahaman [24] that on die compaction, rigid inclusions may cause residual stresses (due to matrix-inclusion mismatch), which reduce the tendency to densify. Furthermore, the random distribution of inclusions obtained by conventional powder mixing procedures can lead to spatial variations in green density within the compact, causing increased differential densification, and therefore a reduced overall densification rate. Experiments performed by Rahaman, however, in which composite powders were compacted to two different green densities [25], that is, at two different uniaxial pressures, revealed no noticeable difference between the sintering behaviour of a powder compacted at high pressures, and one compacted at

relatively low pressures. This seems to suggest that the compaction stage does not introduce appreciable residual stresses, which would be expected to increase with the compaction pressure. Slip casting has been proposed [24] as a desirable alternative to die-compaction, as it is the only technique for ceramic consolidation in which no plastic deformation takes place. However, as demonstrated by Lange, it is very difficult to form bodies by slip-casting, which survive the drying step without the formation of microcracks.

1.1.4. COARSENING EFFECTS

Some of the most recent discussion of the sintering behaviour of composites was by Bordia and Scherer [26], who suggested that the hindrance to complete densification in particulate composites might be attributable to the competition between densification and coarsening mechanisms in the porous body. The proposed origin of the hindrance is as follows: if, as in Figure 1, neck B, (under the influence of the compressive stress σ_r) grows faster than neck A (under the influence of the tensile stress σ_θ), then neck B will reach the required neck size for grain boundary motion sooner and at a lower matrix density than it would in a stress-free matrix. Since the region of matrix near the inclusion undergoes shrinkage in the r- but not in the θ-direction, then coarsening by various mechanisms (such as evaporation-condensation, or surface diffusion) will lead to an increase in the size of neck A, a reduction in neck curvature, and a corresponding decrease in the sintering stress. Furthermore, neck B, by the same mechanisms will either lose its curvature, or the grain boundary at neck A, having attained a certain size, will move from the neck region. In both cases the driving force for densification would be lost.

These neck/grain boundary effects, which would be especially pronounced at the inclusion surface, where $\varepsilon_\theta = 0$, may help to explain why the sintering behaviour of glass-matrix composites roughly obeys the rule of mixtures at low volume fractions [18], whereas that of polycrystalline matrix composites deviates significantly, a problem which most other theories fail to explain. When coarsening occurs, there is an increase in pore size, which reduces the driving force for densification, as the pore surface tension decreases. Two experimental results of Bordia and Raj seem to bear out this idea. First [27], in the TiO_2-Al_2O_3 system, it was found that there is a suppression of the densification rate of the composite with respect to that of pure TiO_2, which is observed from the beginning of densification, and which becomes progressively worse with time (presumably as densification proceeds). Second [28], in hot uniaxial pressing experiments, high densities were achieved only when the uniaxial loads were applied before the sintering temperature was reached, suggesting that the densification rate must be improved during the early stages of sintering; if not, coarsening renders the composite unsinterable at any applied load. Although the matrix grain size is expected to directly affect the densification rate through the densification viscosity, it has already been shown that the reluctance of a composite to densify could not be viscosity related, as, in experiments by DeJonghe and Rahaman [29], the incorporation of inclusions into a ceramic matrix had a profound effect on the densification rate of the matrix material, while the creep rate was unaffected. Since, from equations 2 and 4, both the densification and creep viscosities are expected to be affected in the same way by grain size, it has been inferred that this is not a viscosity-related phenomenon, and that the sintering stress must therefore be dependent on the matrix grain size as well.

1.2 MICROENCAPSULATION AS A SOLUTION

A compound precipitates from solution when the product of the concentrations of the ions involved exceeds the solubility limit of the compound. Hence, according to the La Mer diagram in Figure 2 [29], if one ion is present in solution, and the other is slowly generated, such that its concentration is raised slowly, then, when the threshold of homogeneous nucleation, C(homo) of the compound is exceeded (as in curve "a"), several nuclei of the precipitate should appear simultaneously. In such a situation, the saturation of the solution increases uniformly throughout, as opposed to one in which a solution containing the second ion is mixed with that containing the first, where local variations in concentration may occur. Hence, throughout the solution, several nuclei of homogeneously precipitated material will appear simultaeously. If the peak in the La Mer curve is sharp enough, then nucleation will occur for only a short time before the ion concentration falls below the homogeneous nucleation limit, at which time growth will occur by diffusion. Hence a homogenous powder is obtained.

If preformed solid particles are present, heterogeneous nucleation may occur at lower concentrations. If heterogeneous nucleation is desired, then it is preferable for the behavior of the system to follow curve "c", where a single burst of heterogeneous nucleation occurs, followed by growth, yielding as the product uniform, composite powders. Microencapsulation is expected to provide a solution to the problem of the sintering of composites, as the deposition of the matrix material, or an appropropriate precursor on the surface of the inclusion particulates should eliminate the network formation between non-sinterable inclusions during sintering (at high volume fractions), and the clustering of inclusions (at low volume fractions). Homogeneity within the matrix

should also be improved, as the inclusion phase should be more uniformly distributed, and the particles of the composite powder should be of a narrow size distribution, and therefore pack better.

Curve "b" in Figure 2 is undesirable as a precipitation path, as first heterogeneous, then homogeneous nucleation occurs in the solution. This is undesirable for two reasons. First, one of the main objectives of the coating process is to achieve as high a level of uniformity as possible, when the composite powders are formed into compacts. Homogeneously nucleated matrix material, when present in conjunction with the coated powder, introduces a degree of randomness into the microcomposite. Although this additional matrix material may have only a small randomizing effect in the compact, and the goal of the prevention of interparticle contacts is achieved, purely heterogeneous nucleation, leading to compacts consisting of only coated particles is preferable. Second, it seems that, when homogeneous nucleation begins in such cases, heterogeneous nucleation is arrested, so that, if the core particles are not completely coated at the onset of homogeneous nucleation, complete coverage will not be attained.

Hence, in order to prepare successfully coated powders, four basic considerations are necessary. One must:

(i) Find a technique for the homogeneous precipitation of the matrix material.

(ii) Prepare a stable dispersion of core particles, using a suitable surfacant.

(iii) Ensure that there is an adequate separation between the limits of heterogeneous and homogeneous nucleation, such that only heterogeneous nucleation occurs.

(iv) Vary the concentration of core particles in suspension, in order to find the correct surface area for complete coverage, without also observing homogeneous nucleation.

In addition, a surface treatment may be required to promote nucleation on the preformed cores.

The microencapsulation process has yielded Al_2O_3-SiC_w microcomposites which could be free sintered to very high densities [31]. Coatings have been attempted in the ZnO-SiC system, in which ZnO was heterogeneously nucleated on the surfaces of SiC particulates, following a precipitation reaction devised by Fujita et al [32]. There are many parameters which must be systematically varied in a heterogeneous nucleation system in order to produce acceptable coatings; the temperature, the nature of the anion, the solution pH, the concentration of zinc ions, the concentration of the species which releases the counterion into solution, the concentration of core particles and the reaction time can each be varied to produce zinc oxide crystals of different sizes and morphologies [33], as in Figure 3. Furthermore, when optimal conditions were found for a uniform coating, and the coating is allowed to thicken by crystal growth of the zinc oxide, extensive coarsening and faceting of the coating occurs in solution, rendering the coated particles unsinterable, as shown in Figure 4. In addition, it was found in many cases that the ZnO crystals were deposited as columnar, hexagonal single crystals, which have been shown in other systems [34] to sinter less readily than polycrystalline particles. Thus, it has been found that the microencapsulation technique, which requires a time-consuming set of experiments in order to find the correct coating conditions, does not always yield useful coated powders. Unless complete coverage by heterogeneous nucleation is obtained at the particle surface (for example, using the technique of Bowen et al. [35], in which particle surfaces are

hydrated, then coated by sol-gel techniques), the idea of microencapsulation is probably not a feasible alternative for the production of dense microcomposites.

1.3 DOPING OF MATRIX MATERIAL AS A SOLUTION

In all sintering systems there exists a competition between densification and coarsening processes. Rearrangement of equation 1 gives the densification rate as:

$$\dot{\varepsilon}_d = \frac{\Sigma}{\eta_d(G)} \tag{7}$$

which increases as grain size (or pore size) decreases. Hence, densification provides an incentive for further densification, since, as the pores become smaller (that is, their curvature increases) the rate should increase. On the other hand, as grain size (or pore size) increases, as during coarsening, both the densification rate and the coarsening rate decrease, because the diffusion rates for both processes decrease when the diffusion distance (grain size) increases.

At the same time, it has been shown [27] that one process cannot occur without the other, since, without the surface redistribution process which occurs during coarsening, matter accumulates in the neck region, and impedes densification. However, the kinetics of coarsening are probably much slower than those of densification, as the driving force for interparticle transport by non-densifying mechanisms should be smaller than that for transport to the neck region, as the diffusion distance is larger in the first case. It is therefore expected, for most single phase systems, that densification should dominate the sintering process until the late stages.

The effects of dopants on the sintering behaviour of zinc oxide have been investigated by various authors [37-39]. It is already known that, in the sintering of pure ZnO powders, doping with monovalent cations serves to increase the densification rate, and reduce the sintering temperature [37], whereas doping with trivalent cations tends to have the opposite effect. These findings are taken advantage of in industry in the preparation of varistors, where a small grain size in the sintered piece is beneficial. Aluminum, in particular, has been studied as a dopant [38-40], and has been found to inhibit both densification and coarsening in ZnO. ZnO in the hexagonal wurtzite phase, has been found to contain excess zinc ions in its large interstitial sites [42, 43], the diffusion of which determines the densification rate at high temperatures [44]. Doping, however, leads to the substitution of zinc atoms by aluminum atoms, by the following reaction [41]:

$$Al_2O_3 \xrightarrow{ZnO} 2Al(Zn)^{\cdot} + 2ZnO + 2e' + \frac{1}{2}O_2(g) \qquad (8)$$

The doping of zinc oxide with trivalent elements therefore depletes the concentration of interstitial zinc, thereby decreasing the rates of densification and coarsening (both of which occur by the diffusion of zinc ions) in the early stages of sintering. However, the coarsening rate seems to be affected to a greater extent than the densification rate. This is observed, presumably, because aluminum segregates to the grain surfaces, so that coarsening- probably largely dependent on surface diffusion processes- is hindered more than densification, the grain boundary and lattice diffusion mechanisms of which can still proceed, although at reduced rates. At higher temperatures, probably because of the maintenance of a small grain size (diffusion distance) until the late stages of sintering, the densification and grain growth rates in aluminum-doped powder exceed those of the undoped powders.

The presence of a small concentration of aluminum has also been found [39] to retard creep processes in zinc oxide. While this result may seem, at first, somewhat surprising, it can be explained, as creep processes should be affected by the same phenomena influencing densification and coarsening, since all occur by the same diffusion processes. Thus, the increase in creep vicosity brought about when doping obstructs the diffusion path, overshadows the benefits of keeping the grain size, and hence the diffusion distance small, and no increase in the creep rate is achieved.

The inhibition of coarsening in ceramic matrix composites is expected to prove beneficial for three reasons. First, since creep is essential to the densification of composites, and since the creep rate is known to be inversely proportional either to the square or to the cube of the diffusion distance, the preservation of a small grain size until the later stages of sintering may be expected to improve the creep, and hence the densification behavior. Second, if, as suggested by Lange [22], dense regions develop in the composite which later undergo extensive grain growth, then these regions will resist the creep processes necessary for the further densification of the less dense regions. If, on the other hand, grain growth could be prevented in these areas, the less dense areas would be less constrained, and would be able to lower their free energies by densification, rather than by "desintering". Third, if it is true, as proposed by Bordia and Scherer [26], that the consequences of the constraining action of inclusions are coarsening and a reduced sintering stress, then the inhibition of coarsening would be expected to improve sintering behavior. In any case, a higher endpoint density should be attained in composites in which coarsening is inhibited.

In this work, the effects on sintering of doping the zinc oxide matrix powder with a small amount of aluminum were investigated. Unfortunately, it is not possible to dope the matrix with an ion which inhibits one diffusion process (coarsening), while having no effect on the others (densification and creep). Nevertheless, the study proved very instructive, for the further elucidation of the effects of rigid inclusions on sintering.

2. EXPERIMENTAL PROCEDURE

2.1. POWDER PREPARATION

(i) SiC classification

The silicon carbide powder used in this experiment* was classified to a narrow size distribution (1 to 3 μm) by sedimentation.

(ii) Doped Powders

The ZnO powders used were varistor precursor powders, obtained from Sandia National Laboratory. Their compositions were as follows:

(i) Undoped Powder (Powder "U"): 99.5 mol% ZnO, 0.25 mol% CoO, 0.25 mol% MnO; average particle size: 0.06 μm.

(ii) Al-doped powder(Powder "D"): 99.5 mol% ZnO, 0.25 mol% CoO, 0.25 mol% MnO, 340 ppm Al; average particle size: 0.08 μm.

---

* Norton Company

The co-precipitation techniques used in the preparation of these powders has been described by Dosch et al [44].

Calculated amounts of the 1-3 μm silicon carbide powder were added to the zinc oxide powders so as to obtain doped and undoped powder mixtures containing 1, 5, 10 and 20 vol% of SiC. The powder compositions are denoted hereafter in the following way: the first letter (U or D) describes an undoped or a doped zinc oxide powder. The second letter (U or R) describes whether the powder was unreinforced or reinforced. If reinforced, a number follows the two letters, which represents the volume fraction of silicon carbide in the composite. In each case, the relative amounts of ZnO and SiC required were calculated based on the theoretical density of the resulting composite. Each mixture was stirred magnetically in acetone for at least 24 hours, and ultrasonicated for at least 10 minutes to break up agglomerates of silicon carbide. The powders were then shear mixed at 8000 rpm for 15 minutes, to ensure complete spacial randomness. The mixtures were stir-dried, then vacuum-dried to remove all moisture (which is known to promote coarsening during the sintering of ZnO [45]), then stored in a dessicator.

2.2. COMPACTION

Powders were uniaxially compacted in a 1/4 inch die at a pressure of approximately 6000 psi, to give pellets approximately 0.6cm x 0.6cm, and of the green densities given in Table 1. For each type of powder, green densities were within +/- 0.005 of the average value given in the table.

2.3. SINTERING

Sintering was performed at the constant heating rate of 4 °C/min from room temperature to 1060 °C. At least three compacts were sintered for each powder type and inclusion concentration, and the resulting measurements averaged. The density after sintering was found from geometrical measurements, rather than using the principle of Archimedes, which has been shown to give inaccurate density measurements where open porosity is present.

In addition, the sintering behaviour of the powders containing 5 vol% SiC (undoped and Al-doped) was studied in greater detail using the technique of loading dilatometry [11], and compared with that of the corresponding unreinforced powder. In this set of experiments, compacts were sintered to 1100 °C. For accuracy in comparison of densification rates, the unreinforced powders were compacted to the same *matrix* green density as the reinforced powders, as, in a composite, only the matrix material shrinks during densification. In another set of experiments, the sintering of these powders was stopped at various intermediate temperatures, and the samples were quenched to room temperature from 700, 800, 900, 1000 and 1100 °C, so that the development of density and microstructure could be followed.

3. DATA ANALYSIS

Dilatometry experiments give data for the axial shrinkage of the compact with time; if sintering is performed at a constant heating rate, then axial strain (which is directly

proportional to the voltage change measured by the dilatometer) may be found as a continuous function of the sintering temperature.

The axial strain of a compact during sintering is taken as :

$$\varepsilon_z = ln \frac{z}{z_0} = ln(1 + \frac{\Delta z}{z_0}) \tag{9}$$

where z is the axial length of the sample at any time during sintering, and z_0 is the initial axial length.

Similarly, the radial strain is given by:

$$\varepsilon_r = ln \frac{r}{r_0} \tag{10}$$

where r_0 is the initial radius of the cylindrical compact, and r is the instantaneous value of the radius.

The densification strain was calculated from:

$$\varepsilon_d = \frac{1}{3}(\varepsilon_z + 2\varepsilon_r) \tag{11}$$

The overall radial and axial strains were calculated from dimensional measurements made on the compact before and after sintering. These were used to calculate ε_d. In order

to obtain ε_d as a continuous function of temperature, ε_z was assumed to directly correspond to ε_d during sintering.

Creep strain calculations were performed by the technique of Ghirlanda [38], using the following relation:

$$\varepsilon_c = \varepsilon_z(\sigma) - \varepsilon_d(0) \tag{12}$$

where $\varepsilon_z(\sigma)$ is the axial strain observed under the applied load, σ, and $\varepsilon_d(0)$ is the densification strain obtained under no load. This technique was deemed appropriate in this case, as the application of the small, uniaxial load was not found to have any measureable effect on the endpoint density.

Densification rates and creep rates were obtained from smooth curves fitted to the strain curves, in the following way:

$$\dot{\varepsilon_d} = \alpha \frac{d(\varepsilon_d)}{dT} \tag{13}$$

and

$$\dot{\varepsilon_c} = \alpha \frac{d(\varepsilon_c)}{dT}$$

where α is the constant heating rate of 4 ^{o}C/min. However, since the actual applied stress must increase as the compact shrinks and its cross-sectional area decreases, the creep rate was adjusted in the following way:

$$\dot{\varepsilon_c}(\sigma_0) = \dot{\varepsilon_c}(\sigma) exp(\varepsilon_c - 2\varepsilon_d) \tag{15}$$

where $\dot{\varepsilon}_c(\sigma_0)$ equals the creep rate which would have been obtained under a constant stress of 0.2 MPa.

Density curves were obtained from the following function:

$$\rho = \rho_0 exp(3\varepsilon_d) \tag{16}$$

Densification rate and creep rate curves for doped and undoped samples were further normalized with respect to the similar rates for the unreinforced material, which have been found to be significantly different.

4. RESULTS

The results of the sintering of doped and undoped ZnO with 0 - 20 vol% of silicon carbide, are given in Table 1. The trends in final density and densification strain with volume fraction are shown in Figures 5 and 6. It is interesting to note that in the absence of inclusions, the achieved endpoint density is higher in the undoped than in the doped samples, whereas, even at the lowest volume fraction of silicon carbide (1 vol%), the doped sample attains a higher final density. This small, but consistent improvement in final density and in strain was observed in all reinforced samples. In Figure 7, the normalized densification strain was obtained by dividing the average strain for each powder type by the maximum achievable strain, that is, the strain observed at 0 vol% inclusions. In this plot, the non-trivial improvement in density obtained in the doped powders is clear, the greatest improvement being observed at low volume fractions of inclusions.

In Figures 8 (a) to (e), the microstructures of ZnO-SiC composites containing 0 - 20 vol% SiC are shown. In both doped and undoped samples, significant microstructure coarsening occurs at relatively low volume fractions of SiC (< 5 vol%); however the coarsening occurs to a greater extent in the undoped than in the doped samples. At higher inclusion contents (10 and 20 vol%), both densification and coarsening are so severely inhibited by the presence of the inclusions, that their microstructures are very similar, having a fine grain size, and a porous matrix.

Figures 9 (a) to (e) show the development of microstructure with temperature, in samples containing 5 vol% inclusions, for temperatures between 700 and 1100 ^{o}C. Here, an obvious difference in grain size between doped and undoped samples is seen at higher temperatures ($\geq$ 900 ^{o}C), the aluminum dopant evidently maintaining a finer grain size in the doped sample. In Figure 9 (c), it also seems that the material immediately surrounding the inclusions in the undoped sample coarsens more quickly than that farther away, giving rise to a non-uniform microstructure, whereas in the doped sample, the microstructure is more uniform. In Figure 9(f), the SEM micrograph of an undoped-matrix sample after sintering to 1100 ^{o}C, reveals regions of high density surrounding those of lower density, as described by Lange [22]. Although it is not possible to conclude that the denser regions contain higher concentrations of inclusions than average, extreme grain growth in the vicinity of inclusions is evident. Figure 9(g) is a micrograph of an undoped matrix sample containing 1 vol% of inclusions, showing the presence of void-like damage around inclusions.

Dilatometry results are given in Figures 10-13. In the plots of density and densification strain versus temperature (Figures 10 and 11), it may be seen that, while, in

unreinforced powders, the aluminum dopant has the effect of suppressing the density attained by the doped sample with respect to the undoped sample at any given temperature, the reverse is true in reinforced specimens. Densification rate curves are given versus temperature in Figure 12. Although it is difficult to interpret these rather complicated results, it is obvious that at lower temperatures, the doped-matrix composite has a significantly higher densification rate than the undoped-matrix composite, while at higher temperatures ($\geq$ 1000 ^{o}C), the densification rate in the undoped-matrix powders far surpasses that in the doped. In Figure 13, the normalized densification rate curves show clearly the improvement in densification rate achieved by doping.

Analysis of creep data revealed strains that were very low in comparison with densification strains. As the obtained creep strains were roughly an order of magnitude lower than the axial and densification strains used to calculate them (see Equation 12), they were deemed too low to be quantitatively reliable, and are therefore not included here. However, as will be discussed later, the sintering of loaded composites may be less useful than was previously thought.

5. DISCUSSION

Attempts to interpret the results of these experiments must by made very carefully, as the aluminum dopant does not have the simple effect of retarding coarsening in the matrix, but tends to decrease densification and creep rates as well (see Figure 12).

5.1 MICROSTRUCTURE

Microstructural data obtained from Scanning Electron Microscopy studies could be used only qualitatively. No attempt was made to verify the theory of Bordia and Scherer by grain dimension measurements. If the theory is correct, then the matrix material should experience more grain growth radially outward from the inclusion than in the hoop direction. However, due to the irregular shapes of the inclusions, it was not not possible to determine whether or not this was the case, as radial and hoop directions could not be strictly identified.

It is interesting to note that at 0 and 1 vol% of SiC, the matrix grain size is far greater in the undoped sample, that is, the addition of 1 vol% of inclusions is enough to present a significant impediment to densification, but not to grain growth in undoped samples. A rather surprising result may be seen in Figure 8(c), in which the doped matrix sample attains a slightly higher grain size than the undoped matrix composite. This may be explained by considering two previous experimental findings. First, it was found by Lange et al. [46] that inclusions, when present in low volume fractions, have a negligible effect on grain size, whereas at higher volume fractions, they tend to constrain grain growth in the matrix material. Second, as reported by Ghirlanda [38], the aluminum dopant preserves a low grain size only at low temperatures. At higher temperatures, the fine-grained material probably has a higher driving force for grain growth than its undoped, coarser counterpart, leading to the development of a higher grain growth rate in doped powders than in undoped. In the doped, reinforced sample, at 5 vol% of inclusions, the maintenance of a relatively small grain size (diffusion distance) beyond 1000 ^{o}C has probably generated a higher driving force for both densification and coarsening, than in the undoped, reinforced sample. This, in combination with the grain boundary pinning effects described by Lange, in operation in both samples, probably leads to the slightly higher grain size in the doped

sample. At higher inclusion contents, it seems that not only densification, but also coarsening is inhibited, even in the absence of the aluminum dopant. It is likely that, the presence of a relatively high volume fraction (≥ 10 vol%) of inclusions, where the inclusion size is several times greater than the matrix grain size, has the effect of inhibiting the neck growth and interparticle transport associated with coarsening, in addition to the constraints imposed on densification (see Section 1.3)

In Figure 8(a), an interesting phenomenon can be observed. In the undoped matrix sample, at the ends of the rigid elongated inclusions, densification of the matrix material seems to have occurred without the hindrance of a transient, tensile stress. However, the presence of some transient stress along the edges of the inclusion is evident, as the matrix material at the interface seems to have "desintered"; a void has opened along the length of the inclusion. This suggests that there is some anisotropy in the distribution of stresses, caused by irregularities in the particle shape.

Figures 9(f) and (g) show the effects of differential densification and of void formation, respectively. The causes of these non-uniformities in the sintered microstructures, however, are difficult to ascertain. In Figure 9(f), the regions of very high and very low density may be due to the poor distribution of the inclusion phase obtained by the conventional mixing techniques employed in this experiment, or to the constrained network sintering, and subsequent desintering proposed by Lange. The voids seen encircling inclusions in Figure 9(g) may either be the crack-like voids described by Lange [4], which open in order to dissipate accumulated stresses in the matrix material, or may be due to packing defects initiated during the uniaxial compaction stage. Further

evidence of the constraining effects of the SiC inclusions, even at 1 vol%, is provided by these results.

5.2 LOADING DILATOMETRY

From the plot of density versus temperature for the four types of powder compact (Figure 10), it can be seen that densification is activated at different temperatures in different samples. This is more clearly shown by the densification strain curves, plotted against temperature in Figure 11, in which shrinkage commences in the UU powder at 600 ^{o}C, in the DU powder at 650 ^{o}C, in the DR5 powder at 750 ^{o}C, and in the UR5 powder at 850 ^{o}C. While in the reinforced powders, the aluminum dopant probably serves to obstruct the diffusion path of the Zn^{2+} ion, thereby reducing the densification rate, this inhibiting effect seems to have been absent, or at least less significant in the reinforced powders. That is, the presence of Al^{3+} ions in the reinforced samples allows densification to begin at lower temperatures in the DR5 samples than in the UR5 samples.

At higher temperatures, the UR5 samples attain the same density (and densification strain) as the DR5 samples. Figures 10 and 11 show that, until the highest temperatures are reached, ($\geq$1000 ^{o}C), the density of UR5 is far below that of DR5. The relatively rapid increase in density and densification strain observed in UR5 between 1050 and 1100 ^{o}C, which allows it to "catch up" with DR5 is probably related to the coarsening effect discussed earlier (Section 5.1).

While the inhibition of coarsening in the composite has not served to completely eliminate the hindrance to sintering caused by rigid inclusions (that is, the DR5 samples do

not attain the same final density as the UU or DU samples), it is obvious that some benefit has been derived from the presence of dopant. The doped matrix composites were observed to maintain a higher density and densification rate than the undoped matrix composites until the very end of sintering (approaching 1100 ^{o}C). This is significant, since it is generally desireable to perform sintering at the lowest possible temperatures, because of economical considerations, and in order to prevent the matrix and inclusion phases from reacting with each other.

As would be expected from the density and densification strain curves in Figures 10 and 11, each of the four types of powder has a very different curve of densification rate versus temperature from the others (see Figure 12). Although the plot seems rather complicated and difficult to interpret, certain aspects may be mentioned. First, the maxima in the rate curves occur at roughly the same temperature ($\approx$ 800 ^{o}C) for both unreinforced powders, and at approximately the same temperature ($\approx$ 1050 ^{o}C) in both reinforced powders. Thus, the addition of inclusions has had the effect of delaying densification in both powders, causing the maximum rate to be reached at higher temperatures. This delay in the onset of densification and in the attainment of maximum densification rate implies different activation energies in the reinforced than in the unreinforced materials. However, results of EDAX, X-Ray Diffraction and Auger Electron Spectroscopy experiments failed to indicate the presence of any impurities in appreciable amounts in composite powder mixtures or in sintered pieces (see Figures 14 and 15). Traces of chloride impurities ($\approx$ 1 atomic percent) were discovered in both reinforced and unreinforced samples which fails to account for the shift in the densification curves. Second, at temperatures below approximately 1000 ^{o}C, the densification rate is significantly higher in the doped, reinforced samples than in the undoped reinforced samples, although in the unreinforced powder, the reverse is true. This suggests that the increased driving force for densification

obtained by the maintenance of a small matrix grain size is enough to overcome the reduction in driving force which occurs when the diffusion path for zinc ions is obstructed. Furthermore, it proves that the hindrance to densification may be, to a great extent, overcome by the inhibition of coarsening in the early stages of sintering. At about 1000 ^{o}C, the rate curves for the two reinforced samples intersect; thereafter, there is a sharp increase in the densification rate of the UR5 specimens. The failure of the DR5 powders to attain such a high densification rate may be due to the obstruction of the diffusion path introduced by the dopant ions, or to the competition between densification and the rapid coarsening occuring above 1000 ^{o}C. Simultaneous examination of Figures 9 (d) - (e) and Figure 13 indicates that between 1000 and 1100 degrees, where the coarsening rate is evidently much greater in DR5 than in UR5 samples, the densification rate in DR5 samples is correspondingly lower than that in DR5 samples.

Since, in unreinforced powders, the aluminum dopant has the effect of reducing densification rate at low temperatures, it is perhaps more instructive to examine the graph of normalized densification rate versus density (Figure 13). In these curves, the densification rate in each type of reinforced powder is given as a fraction of the densification rate of the corresponding unreinforced powders (which is assumed to be the maximum rate attainable by the matrix material for that type of powder). In UR5 powders, the normalized rate is virtually zero below 850 ^{o}C, at which temperature densification begins. As can be seen from the figure, the normalized rate in the UR5 powder is significantly less than that in the DR5 powder at temperatures below approximately 950 ^{o}C. The presence of the aluminum dopant has therefore allowed the doped matrix composites to more closely approach the behaviour of the corresponding unreinforced powder. The normalized rates for both powders increases with temperature. Thus it seems that the densification rate of the

composite more closely approaches that of the unreinforced matrix material at higher temperatures. It also seems that the presence of the dopant has allowed the DR5 composite to maintain greater microstructural uniformity at lower temperatures, which is reflected in the normalized rate. Above 950 ^{o}C, both normalized rates increase sharply, their values exceeding unity, because the densification of the unreinforced powders is nearly completed, so that the densification rates of UU and DU powders fall, while those of UR5 and DR5 are increasing.

In order to adequately explain the aluminum dopant's effect on the sintering behavior of ZnO-SiC composites, two possiblities must be considered. First, the control of coarsening, and hence the retention of a fine matrix grain size until the later stages of densification could promote creep in locally dense regions, relieving any backstresses which may oppose densification. Second, as discussed by Shaw and Brook [46], the aluminum additive may serve to stabilize the matrix microstructure, by restraining such processes as abnormal grain growth, giving rise to a greater degree of uniformity in the compact without the opening of voids, and therefore reducing the exent of differential densification. Experimental data obtained in the present work indicate that an explanation of the improvement in sintering behavior on doping can probably be obtained from the former theory, where the backstresses generated in the matrix give rise to local shear stresses, and the rate of diffusional creep, which varies as $1/d^2$ (Nabarro-Herring creep) or $1/d^3$ (Coble creep) is higher in samples in which coarsening has been prevented at low temperatures.

5.3 A MODIFICATION TO THE CURRENT SINTERING THEORY

A plausible explanation of the effects on densification rate of doping the matrix material in a ceramic matrix composite with a grain growth inhibitor may be derived from the following. All sintering bodies may be considered as consisting of at least two phases: solid material and porosity. There is therefore some degree of inhomogeneity in all sintering systems, and local deformation, or shear, must always occur in order for full or near-full densities to be achieved. However, the sintering theory which has thus far been derived from considerations of a homogeneous, inclusion-free material, in which the pore phase forms a readily deformable network of low shear viscosity, may not be applicable to systems in which a sinterable matrix material is reinforced with a non-sinterable network of inclusions which is resistant to shear deformation. The results of experiments in which composites are sintered under applied uniaxial loads must now be re-examined, as two shear viscosities may be described for the sintering composite- a global shear viscosity representing the ability of the inclusion network to be deformed under the influence of the applied load, and a local shear viscosity, representing the ease with which localized regions of the network can creep in response to the transient stresses generated during densification. When sintering is performed under an applied uniaxial load that has no measureable effect on the densification rate, then it can be assumed that the applied stress serves to facilitate the shear deformation of the stiff inclusion network, while having no effect on the driving force for sintering. Some local matrix densification may be required in order to accommodate the shear of the stiff inclusion network, however. Whereas during free sintering, knowledge of the ratio of densification viscosity to the viscosity associated with local network shear deformation processes may be used to infer the magnitude of the sintering stress, the application of a uniaxial load leads to a global network shear at constant

volume. Hence, it is likely that the network of inclusions undergoes deformation under an applied load by a different mechanism than that for local creep induced during free sintering. Therefore, there is probably no simple relationship between the global creep viscosity obtained by sintering under applied load and the network densification viscosity, such that the creep-sintering behavior of composites cannot be described in terms of Equations (1) and (3).

The network of rigid inclusions present in a composite should have a greater load-bearing capacity than the surrounding matrix material. The magnitude of this capacity may be represented by a network shear viscosity, μ_n, while the ability of the matrix material to support an applied stress is given by μ_m. Deformation compatibility requires that the shear rates of matrix and inclusion network be equal. Hence:

$$\dot{\varepsilon}_s = \frac{\sigma_m}{\mu_m} = \frac{\sigma_n}{\mu_n} \qquad (17)$$

where, due to the higher value of network shear viscosity than matrix shear viscosity, partitioning of the applied stress between inclusion network and matrix occurs, such that the hydrostatic stress component of the applied uniaxial stress in the matrix, σ_m may not be 1/3 of the applied stress, but could be much lower.

If each network element is rigid and undeformable, it would be expected to have a profound effect on densification and shear behavior. As shown in Figure 16 [48], it is to be expected that matrix shear around a rigid inclusion would be more difficult than matrix shrinkage around that inclusion. It is therefore likely that the network will have a far higher

shear viscosity than densification viscosity. If we let the inclusion network volume fraction equal f, then the densification rate of the composite may be described by:

$$\dot{\varepsilon}_d = \frac{\Sigma_m}{(1-f)\eta_m + f\eta_n} \tag{18}$$

where Σ_m = matrix sintering stress,

η_m = densification viscosity of the matrix material.

η_n = shear viscosity of the matrix material.

The creep behavior under uniaxial load may be described by an equation analogous to that for densification:

$$\dot{\varepsilon}_c = \frac{\sigma}{(1-f)\mu_m + f\mu_n} \tag{19}$$

and the ratio of densificaiton rate to creep rate is given by:

$$\frac{\dot{\varepsilon}_d}{\dot{\varepsilon}_c} = \frac{\Sigma_m}{\sigma} \cdot \frac{(1-f)\mu_m + f\mu_n}{(1-f)\eta_m + f\eta_n} \tag{20}$$

Assuming that $\eta_n \gg \eta_m$, and that $\mu_n \gg \mu_m$, the expression for the rate ratio reduces to:

$$\frac{\dot{\varepsilon}_d}{\dot{\varepsilon}_c} = \frac{\Sigma_m}{\sigma} \cdot \frac{\mu_n}{\eta_n} \tag{21}$$

Since there is no simple way to relate the ratio of network creep viscosity to network densification viscosity, as they are probably related to different diffusion mechanisms, it is no longer possible to assume that such a ratio remains constant throughout the sintering process. The magnitude of the sintering stress, therefore, cannot be inferred from the ratio of densification rate to creep rate, as variations in the viscosity ratio would cause a misleading variation in the rate ratio, even at a constant value of Σ. Thus, the formation of this constraining network, as suggested by Lange, may be expected to have a profound effect on the densification behavior of the composite, through the inhibition of shear deformation.

Further evidence of the importance of this constraining network is provided by the following experimental results:

(i) As seen in the current study, sintering behavior is improved in composites in which the matrix material has been doped with a grain growth inhibitor, although the presence of the dopant is known to obstruct the diffusion path of the zinc ions which determine the densification rate. The inhibition of coarsening, and therefore the conservation of a fine grain size in the matrix, compensates for this reduction in the rate of diffusional transport, by improving the rate of diffusional creep. This effect should be especially pronounced when the sintering behavior of glass matrix composites is compared with that of polycrystalline ceramic composites in which the matrix grain size is large, and therefore difficult to deform by diffusional creep.

(ii) Glass matrix composites, in which viscous flow readily occurs, can be sintered to higher densities than ceramic matrix composites containing the same volume fraction of

inclusions, in which creep occurs by diffusional mechanisms [17]. Since the ability of a composite to densify depends heavily on its abilty to deform in response to local stresses, systems in which shear deformation occurs easily should show improved densification behavior over those in which shear is constrained by the network.

(iii) Microencapsulation of inclusions with matrix material improves uniformity and the resulting sintering behavior of composites [30]. In this case, inclusions are probably prevented from forming the extended networks of high shear viscosity, thereby improving the global creep ability of the composite and promoting densification.

6. CONCLUSIONS

The effects on the sintering behavior of ceramic matrix composites of doping the matrix with a grain growth inhibitor have been investigated. The presence of the dopant was found to modify the microstructure of the composite, and to have a strong influence on the densification and creep rates. The dopant was shown to preserve a finer, more uniform microstructure during sintering in doped matrix composites than is found in undoped matrix composites. The presence of the aluminum dopant was found to maintain a fine matrix grain size until the late stages of sintering only in composites containing a low volume fraction of inclusions ($\leq$ 5 vol%). At higher volume fractions, both densification and coarsening were inhibited in the doped matrix composite, as in all ceramic matrix composites.

As expected, the reinforced powders achieved a significantly lower endpoint density than unreinforced powders, with the DR powders attaining higher endpoint

densities than the UR powders. The reinforced powders densified far more slowly than the unreinforced, with the densification of UR5 powders being significantly delayed until very high temperatures. Examination of the sintering behavior of unreinforced compacts of undoped and Al-doped zinc oxide revealed that the presence of the dopant inhibits densification. However, the observed densification strain and strain rate of the doped, reinforced powders were depressed less with respect to the doped, unreinforced powders, than were the undoped reinforced powders in comparison with the undoped, unreinforced powders . This implies that, although the densification is impeded by the presence of the aluminum dopant, the improved shear behavior obtained by the preservation of a fine matrix grain size is able to improve densification behavior.

Finally, a modification to the current theories of sintering was suggested, in which the theories of sintering derived for single-phase systems are inapplicable to composite systems, so that creep-sintering experiments may not be used to determine the sintering stress.

7. REFERENCES

1. W. H. Rhodes, "Agglomerate and Particle Size Effects on Sintering Yttria-Stabilized Zirconia", *J. Am. Ceram. Soc.* **64** [1] 19-22 (1981).

2. F. W. Dynys and J. W. Halloran, "Influence of Aggregates on Sintering", *J. Am. Ceram. Soc.* **67** [9] 596-601 (1984).

3. R. L. Pober, E. A. Barringer, M. V. Parish, N. Levoy and H. K. Bowen, "Dispersion and Packing of Narrow Size Distribution Ceramic Powders", *Materials Science Research* **17** 193-206 (1984).

4. F. F. Lange and M. Metcalf, "Processing-Related Fracture Origins: II, AgglomerateMotion and Cracklike Internal Surfaces Caused by Differential Sintering", *J. Am. Ceram. Soc.* **66** [6] 398 (1983).

5. L. C. De Jonghe and M. N. Rahaman, C. H. Hsueh, "Transient Stresses in Bimodal Compacts during Sintering", *Acta Metall.* **34** [7] 1467-1471 (1986).

6. R. Raj and R. K. Bordia, "Sintering Behavior of Bi-Modal Powder Compacts", *Acta Metall.* **32** [7] 1003-1019 (1984).

7. W. H. Tuan, E. Gilbart and R. J. Brook, "Sintering of Heterogeneous Ceramic Compacts", *J. Mat.Sci.* **24** 1062-1068 (1989).

8. C. H. Hsueh, A. G. Evans, R. M. Cannon and R. J. Brook, "Viscoelastic Stresses and Sintering Damage in Heterogeneous Powder Compacts", *Acta Metall.* **34** [5] 927-93 (1986).

9. L. C. De Jonghe and M. N. Rahaman, "Sintering Stress of Homogeneous and Heterogeneous Powder Compacts", *Acta Metall.* **36** [1] 223-229 (1988).

10. R. L. Coble, "A Model for Boundary Diffusion Controlled Creep in Polycrystalline Materials", *J. Appl. Phys.* **34** [6] 1679-1682 (1963).

10. A. G. Evans, "Considerations of Inhomogeneity Effects in Sintering", *J. Am. Ceram. Soc.* **65** [10] 497-501 (1982).

11. L. C. De Jonghe and M. N. Rahaman, "Loading Dilatometer", *Rev. Sci. Instrum.* **55** [12] 2007-2010 (1984).

12. M. N. Rahaman and L. C. De Jonghe, "Sintering of CdO Under Low Applied Stress", *J. Am. Ceram. Soc.* **67** [10] C205-207 (1984)

13. M. N. Rahaman and L. C. De Jonghe, "Effect of Shear Stress on Sintering", *J. Am. Ceram. Soc.* **69** [1] 53-58 (1986).

14. C. H. Hsueh, "Sintering Behavior of Powder Compacts with Multiheterogeneities", *J. Mat. Sci.* **21** 2067 (1986).

15. C. H. Hsueh, A. G. Evans and R. M. McMeeking, "Influence of Multiple Heterogeneities on Sintering Rates", *J. Am. Ceram. Soc.* **69** [4] C64-66 (1986).

16. G. W. Scherer, "Sintering with Rigid Inclusions", *J. Am. Ceram. Soc.*, **70** [10] 719-725 (1987).

17. M. N. Rahaman and L. C. De Jonghe, "Effect of Rigid Inclusions on the Sintering of Glass Powder Compacts", *J. Am. Ceram. Soc.* **70** [12] C348-351 (1987).

18. R. K. Bordia and R. Raj, "Analysis of Sintering of a Composite with a Glass or Ceramic Matrix", *J. Am. Ceram. Soc.* **69** [3] C55-57 (1986).

19. F. F. Lange, "Constrained Network Model for Predicting Densification Behavior of Composite Powders", *J. Mater. Res.* **2** [1] 59-65 (1987).

20. F. F. Lange, D. C. C. Lam and O. Sudre, "Powder Processing and Densification of Ceramic Composites", *Mat. Res. Symp. Proc.* **155** [4] 81-89 (1986).

21. O. Sudre, D. C. C. Lam and F. F. Lange, "Densification Behavior of Al_2O_3 Powder Containing ZrO2 Inclusions", *Mat. Res. Symp. Proc.* **155** [4] (1989).

22. F. F. Lange, "Densification of Powder Rings Constrained by Dense Cylindrical Cores", *Acta Metall.*, **37** [2] 697-704 (1989).

23. L. C. De Jonghe and M. N. Rahaman, "Densification of Particulate Ceramic Composite: the Role of Heterogeneities", *Mat. Res. Symp. Proc.* **155** [4] 353-361 (1986).

24. M. N. Rahaman and L. C. De Jonghe, "Sintering of Particulate Ceramic Composites: Effect of Matrix Density", Submitted to the J. Am. Ceram. Soc.

25. R. K. Bordia and G. W. Scherer, "On Constrained Sintering- III. Rigid Inclusions", *Acta Metall.* **36** [9] 2411-2416 (1988).

26. R. K. Bordia and R. Raj, "Sintering of TiO2-Al203 Composites: A Model Experimental Investigation", *J. Am. Ceram. Soc.*, **71** [4] 302-310 (1988).

27. R. K. Bordia and R. Raj, *Adv. Ceram. Mater.*, **3** [2] 122-126 (1988).

28. M. N. Rahaman and L. C. De Jonghe, "Sintering of Particulate Composites Under a Uniaxial Stress", Submitted to the J. Am. Ceram. Soc.

29. V. K. La Mer and R. H. Dinegar, "Theory, Production and Mechanism of Formation of Monodispersed Hydrosols", *J. Am. Chem. Soc.* **72** [11] 4847-4854 (1950).

30. T. Mitchell, D. Kapolnek and L. DeJonghe, "Alumina-SiC Whisker Composites from Coated Powders", Paper No. 30-SIV-90, American Ceramic Society 92nd Annual Meeting, Dallas, April, 1990

31. K. Fujita and I. Kayama, "Preparation of Zinc Oxide by the Homogeneous Precipitation Method", *Funtai Oyobi Funmatsi Yakin* **28** [1] 33-34 (1981)

32. G. Brown, unpublished results, 1990

33. E. B. Slamovich and F. F. Lange, "Densification Behavior of Single Crystal and Polycrystalline Spherical Particles of ZrO2 made by Electrostatic Atomization",

34. H. Okamura, E. A. Barringer, H. K. Bowen, "Preparation and Sintering of Narrow-Sized Al_2O_3-TiO_2 Composite Powders, *J. Mat. Sci 24* 1867-1880 (1989).

35. F. F. Lange, "Contributions of Sintering and Coarsening to Densification of Crystalline Powders", F. F. Lange

36. A. M. R. Senos, M. R. A. Santos and J. M. Vieira, "Effects of Particle Rearrangement on Sintering of ZnO Fine Powders", *Science of Ceramics* **14** 265-271 (1989).

37. K. M. Kimball and D. H. Doughty, "Aluminum Doping Studies on High Field ZnO Varistors", SANDIA Report 86-0713 (1987).

38. M. Ghirlanda, MS Thesis, U. C., Berkeley, 1990

39. W. G. Carlson and T. K. Gupta, "Improved Varistor Nonlinearity Via Donor Impurity Doping", *J. Appl. Phys.*, **53** [8] 5746-5753 (1982).

40. W. Komatsu, M. Miyamoto, S. Hujita and Y. Moriyoshi, "Effects of Dopants on Sintering of ZnO and NiO", *Yogyo Kyokaishi* **76** [12] 407-412 (1968).

41. F. A. Kroger, "The Chemistry of Imperfect Crystals", North Holland, Amsterdam (1964).

42. M. H. Sukkar and H. L. Tuller, *Advances in Ceramics* **7** 71 (1982).

43. T. K. Gupta and R. L. Coble, "Sintering of ZnO: I, Densification and Grain Growth" *J. Am. Ceram. Soc.* **51** [9] 521-525 (1968).

44. R. G. Dosch, B. A. Tuttle, R. A. Brooks, "Chemical Preparation and Properties of High-Field Zinc Oxide Varistors",*J. Mater. Res.* **1** [1] 90-99 (1986)

45. P. Q. Mantas and J. L. Baptista, "Effect of Residual Moisture on the Sintering and Electrical Characteristics of ZnO Varistors", *Science of Ceramics* **14** 985-989 (1989)

46. N. J. Shaw and R. J. Brook, "Structure and Grain Coarsening During the Sintering of Alumina", *J. Am. Ceram. Soc.* **69** [2] 107-110 (1986).

47. M. Y. Chu, Phd Dissertation, (1990).

48. L. C. De Jonghe, private communication, 1990.

Powder Type	UU	UR1	UR5	UR10	UR20
Initial Densit	0.465	0.475	0.469	0.49	0.51
Final Density	0.945	0.723	0.639	0.618	0.567
Axial Strain	0.244	0.153	0.106	0.092	0.047
Radial Strain	0.246	0.153	0.112	0.087	0.045
Dens. Strain	0.245	0.153	0.11	0.089	0.045
Powder Type	DU	DR1	DR5	DR10	DR20
Initial Densit	0.468	0.474	0.478	0.492	0.507
Final Density	0.891	0.755	0.661	0.651	0.586
Axial Strain	0.219	0.178	0.136	0.108	0.063
Radial Strain	0.22	0.166	0.121	0.1	0.058
Dens. Strain	0.219	0.17	0.126	0.103	0.059

Table 1: Results of sintering doped and undoped ZnO containing 0 - 20 vol% SiC.

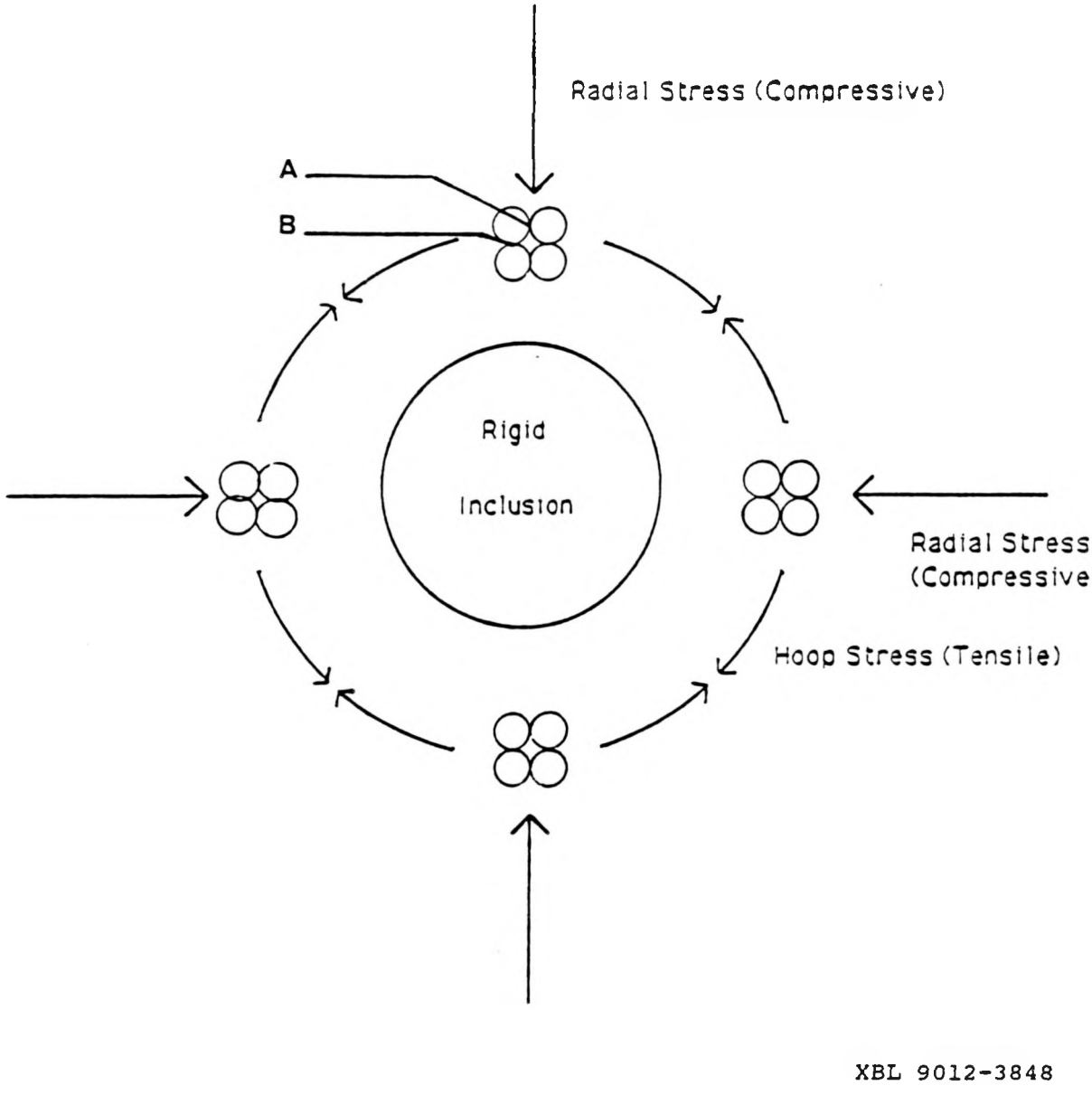

Figure 1: Schematic diagram showing development of stresses around a rigid inclusion during sintering, as suggested by Bordia and Scherer [25].

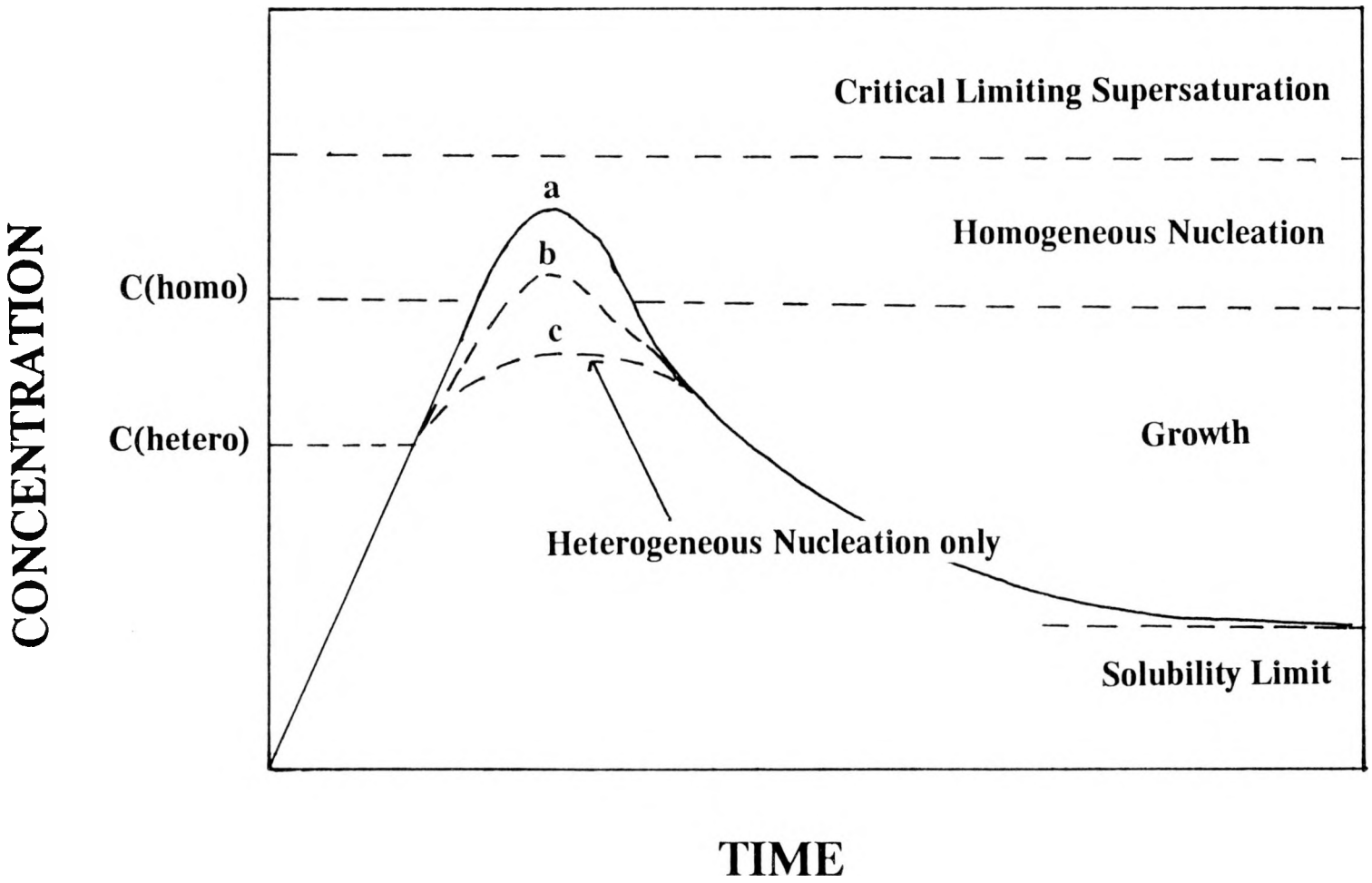

Figure 2: La Mer diagram [29].

a

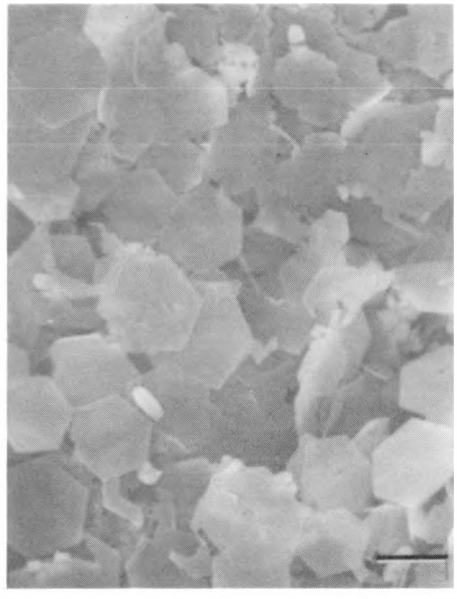

b

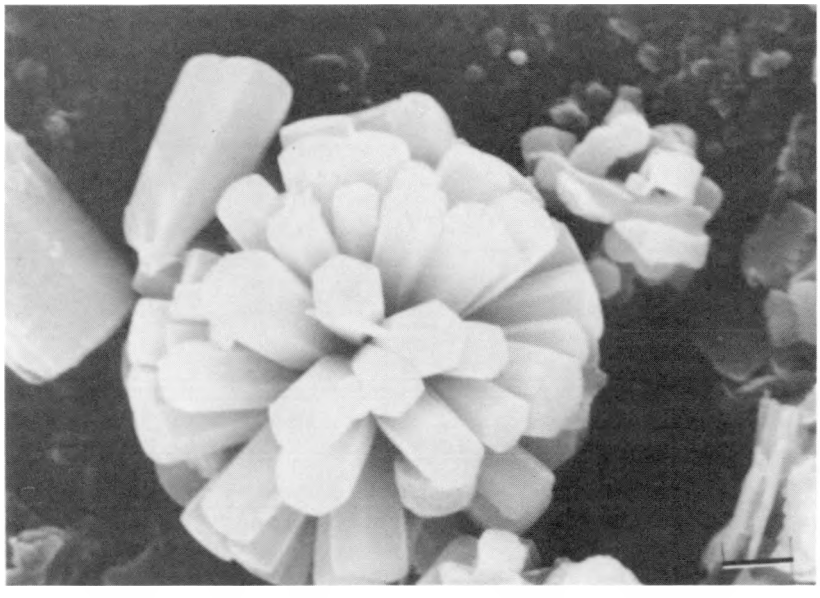

c

Figure 3: Zinc oxide crystals produced under different experimental conditions.
(a) Bar = 2.4 μm. (b) Bar = 2.7 μm. (c) Bar = 662 nm.

XBB 911-350

Figure 4(a): ZnO-SiC, from nitrate solution, after 15 minutes. Bar = 3.3 μm.

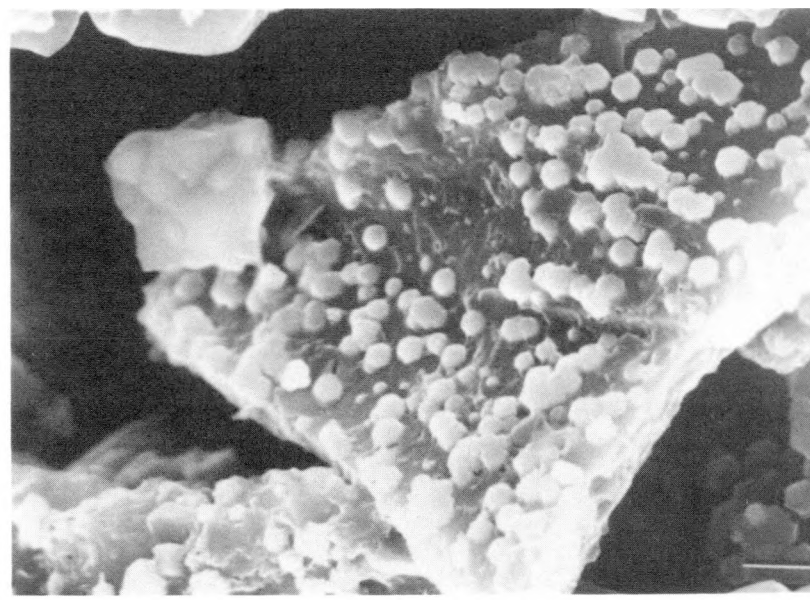

Figure 4(b): ZnO-SiC, from nitrate solution, after 30 minutes. Bar = 1.66 μm

XBB 911-342

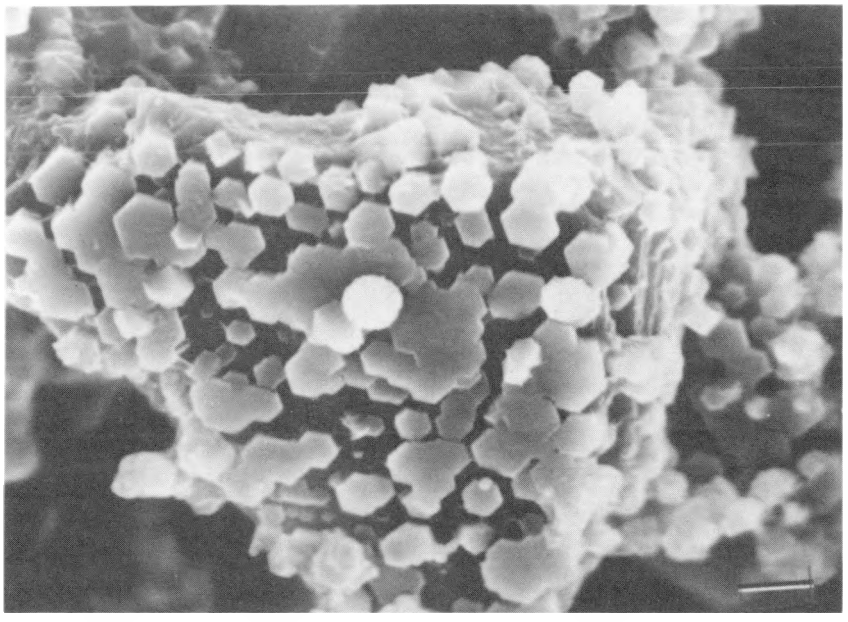

Figure 4(c): ZnO-SiC, from nitrate solution, after 45 minutes. Bar = 1.66 μm.

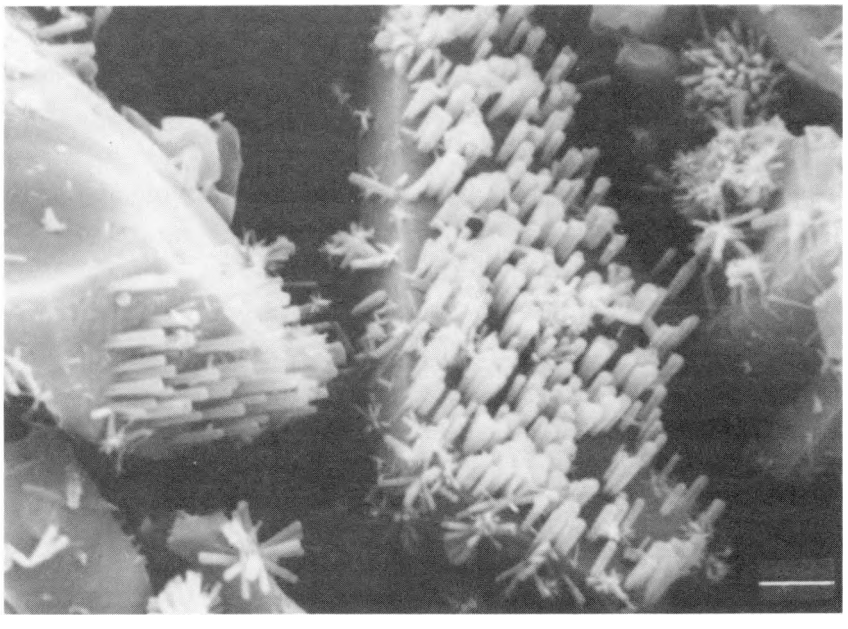

Figure 4(d): ZnO-SiC, from chloride solution, after 40 minutes. Bar = 1.91 μm

XBB 903-1980A

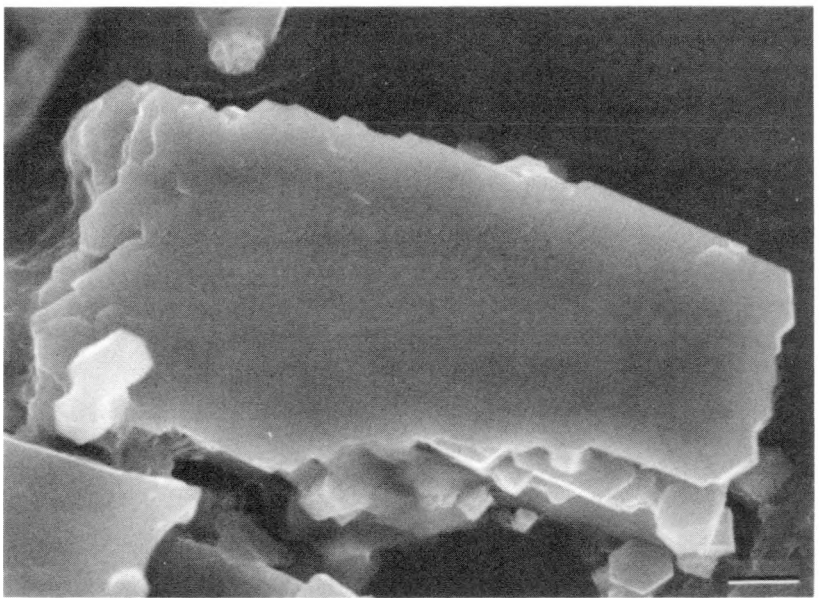

Figure 4(e): ZnO-SiC, desired coating quality obtained, low volume fraction of ZnO.
Bar = 1.66 mm

XBB 911-348

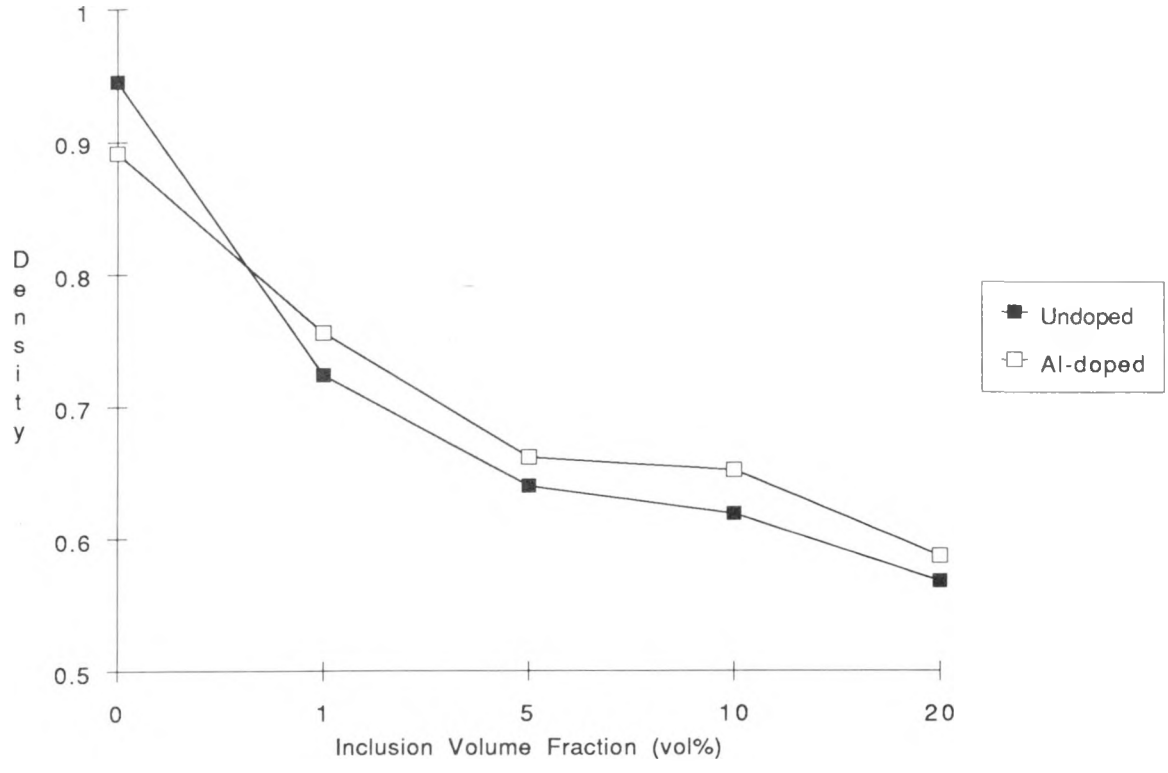

XBL 911-49

Figure 5: Graph of final density of Zn0-SiC composites versus volume fraction of inclusions.

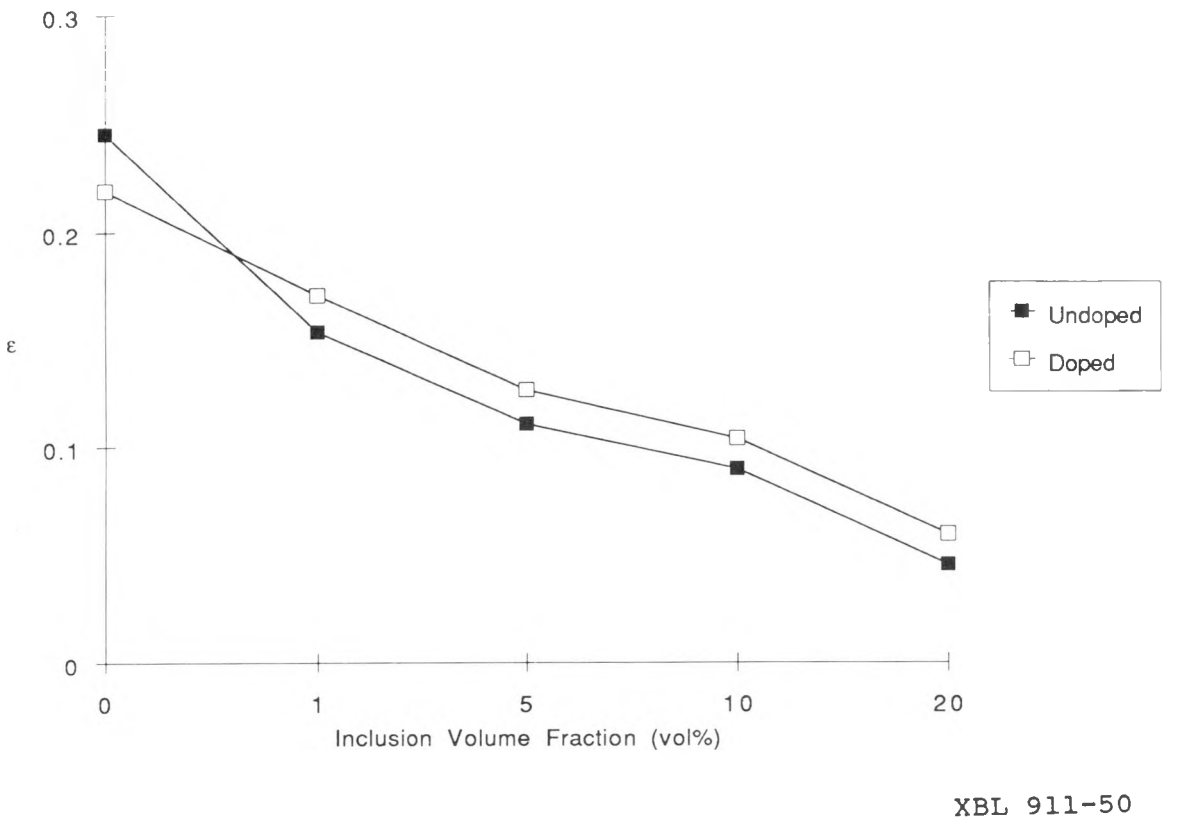

Figure 6: Graph of densification strain in Zn0-SiC composites versus volume fraction of inclusions.

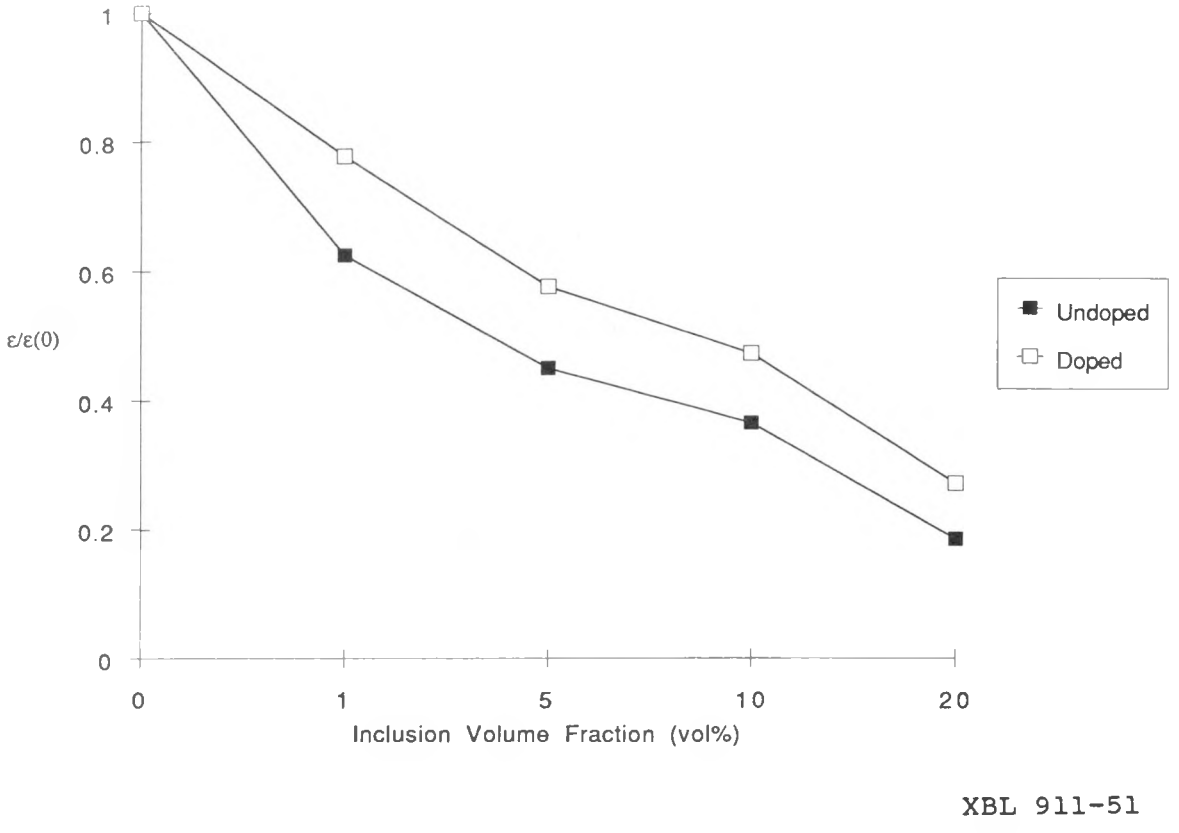

Figure 7: Graph of normalized densification strain in Zn0-SiC composites versus volume fraction of inclusions.

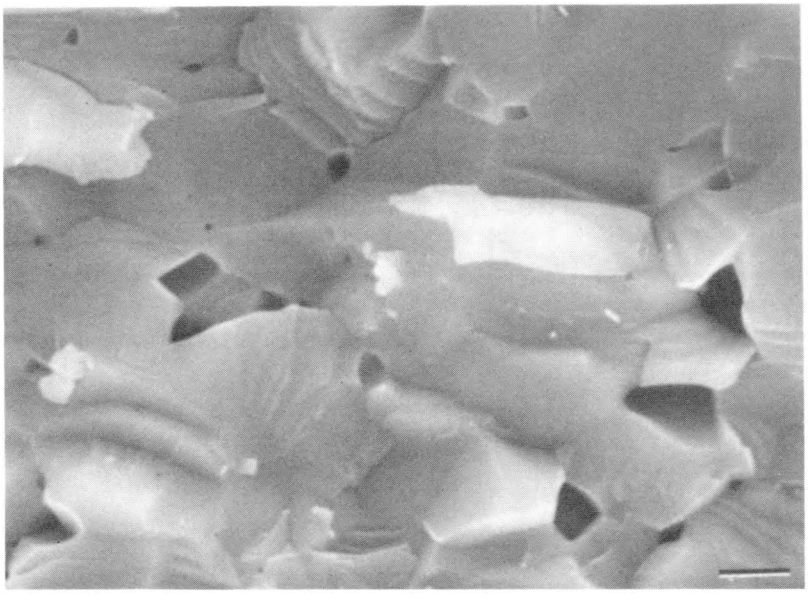

Undoped, unreinforced ZnO, sintered to 1100 °C.

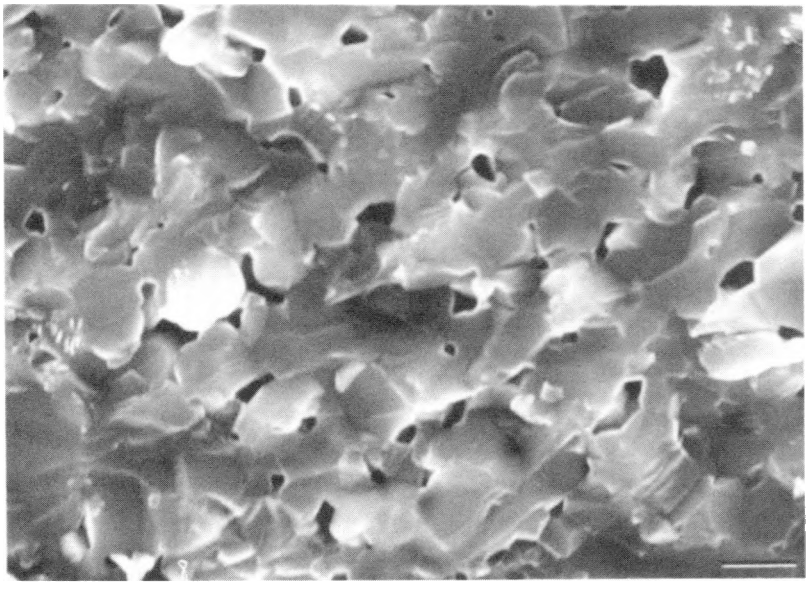

Doped, unreinforced ZnO, sintered to 1100 °C.

Figure 8(a): Bar = 1 μm XBB 911-341

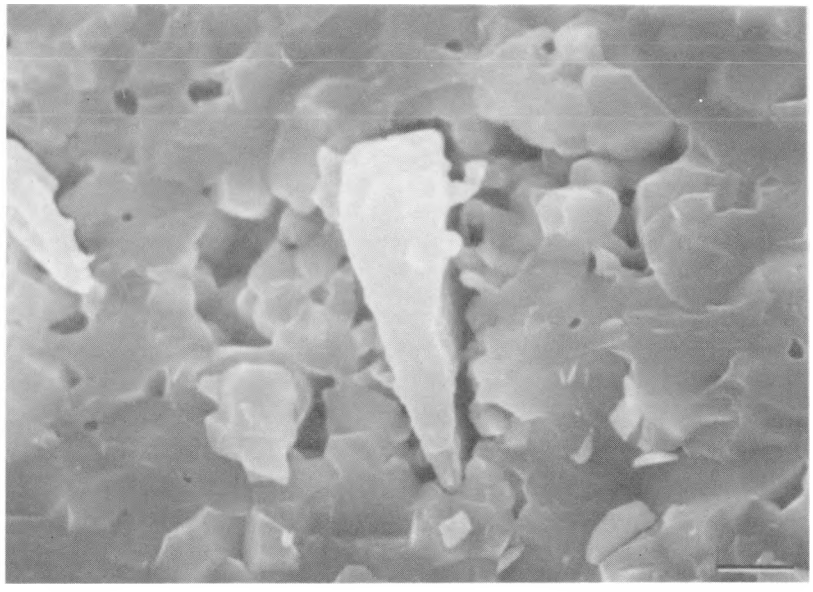

Undoped matrix, 1 vol% SiC, sintered to 1100 °C.

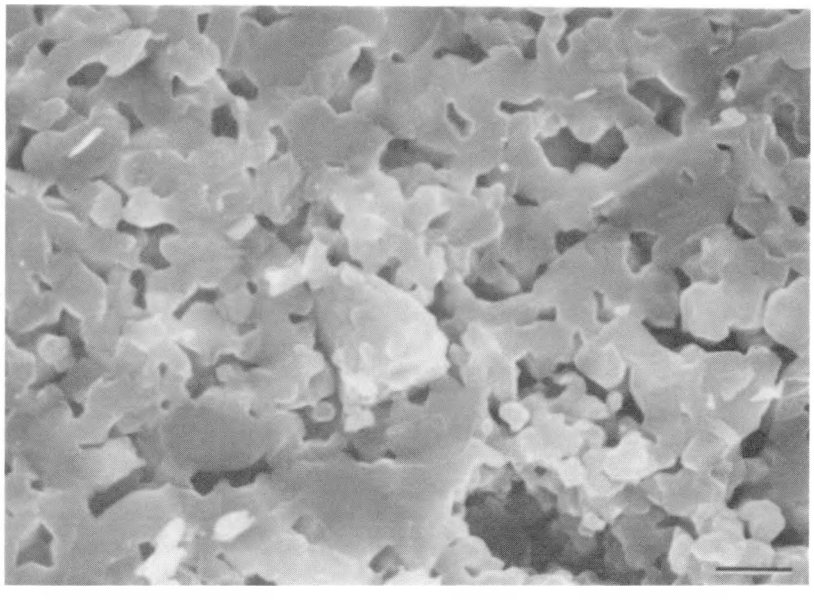

Doped matrix, 1 vol% SiC, sintered to 1100 °C.

Figure 8 (b): Bar = 1μm. XBB 911-339

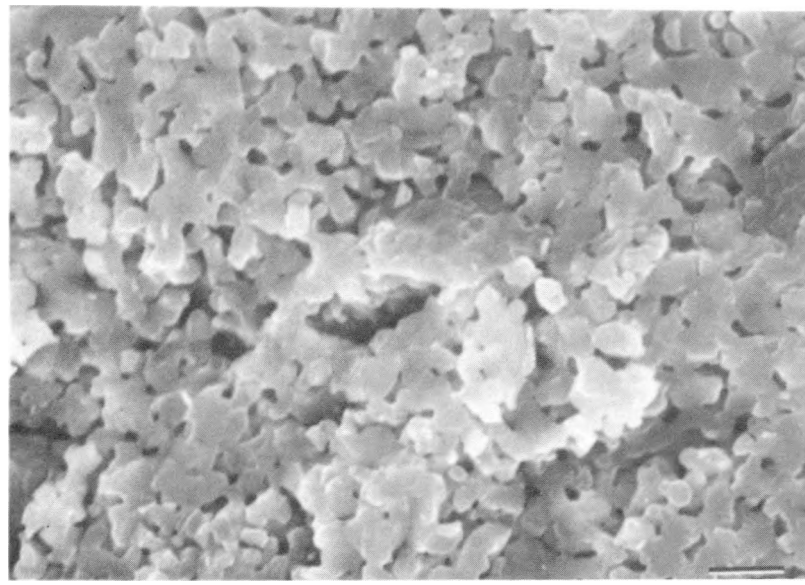

Undoped matrix, 5 vol% SiC, sintered to 1100 °C.

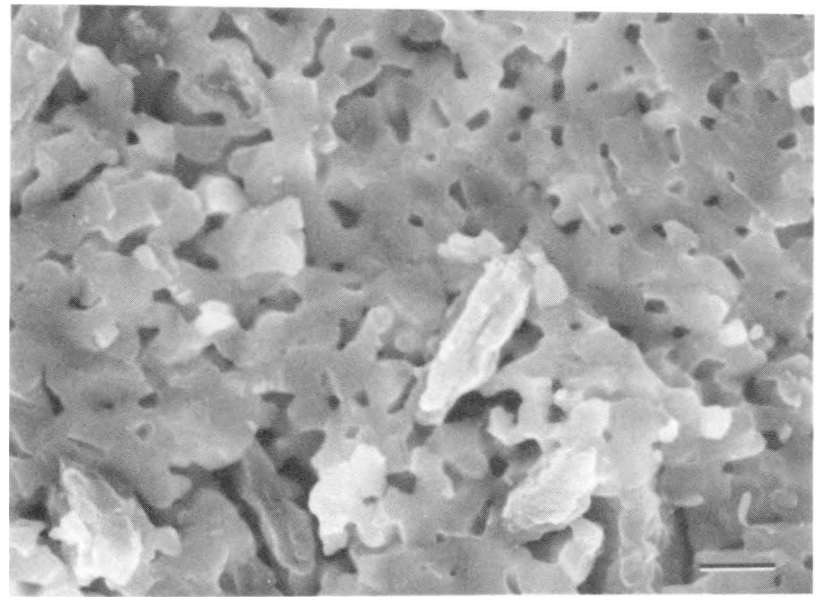

Doped matrix, 5 vol% SiC, sintered to 1100 °C.

Figure 8(c): Bar = 1 μm

XBB 911-340

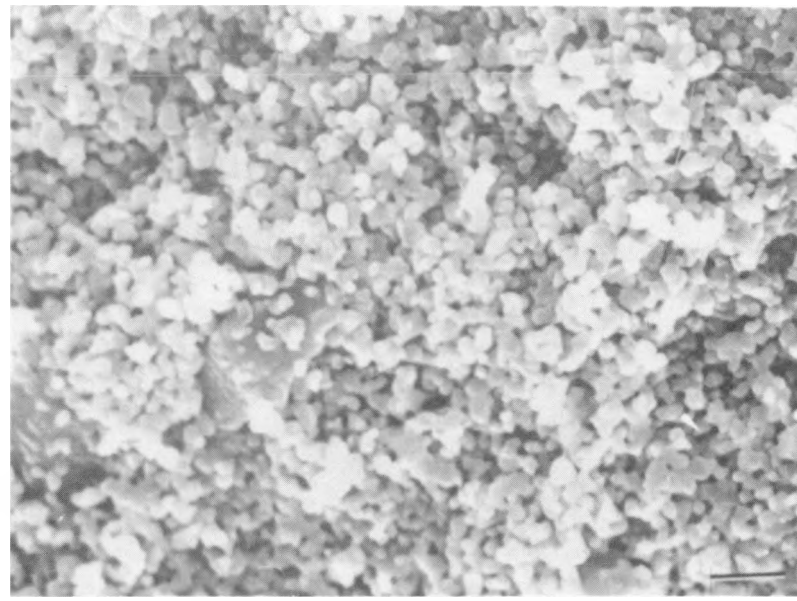

Undoped matrix, 10 vol% SiC, sintered to 1100 °C.

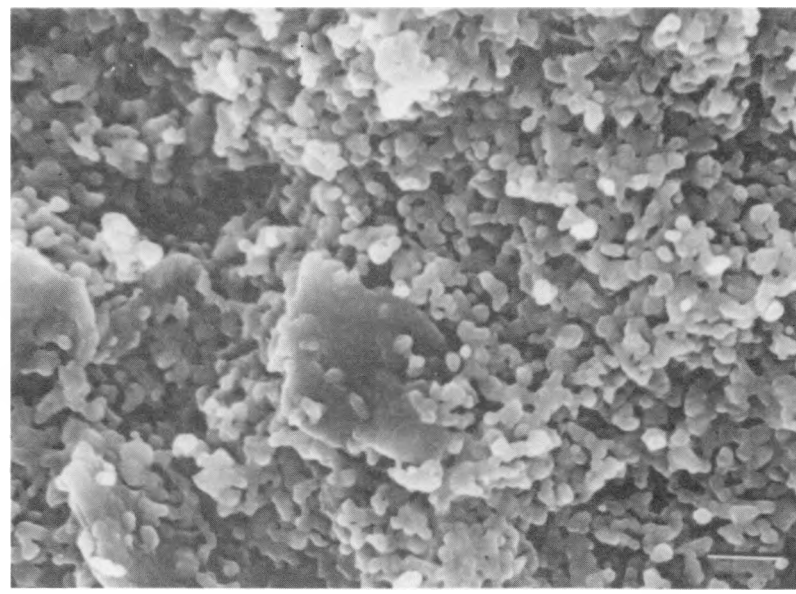

Doped matrix, 10 vol% SiC, sintered to 1100 °C.

Figure 8(d): Bar = 1μm XBB 911-338

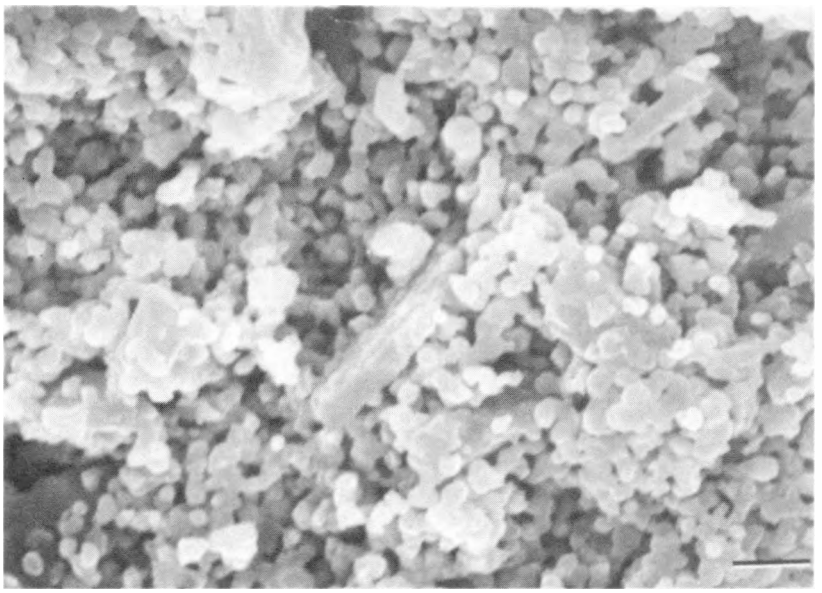

Undoped matrix, 20 vol% SiC, sintered to 1100 °C.

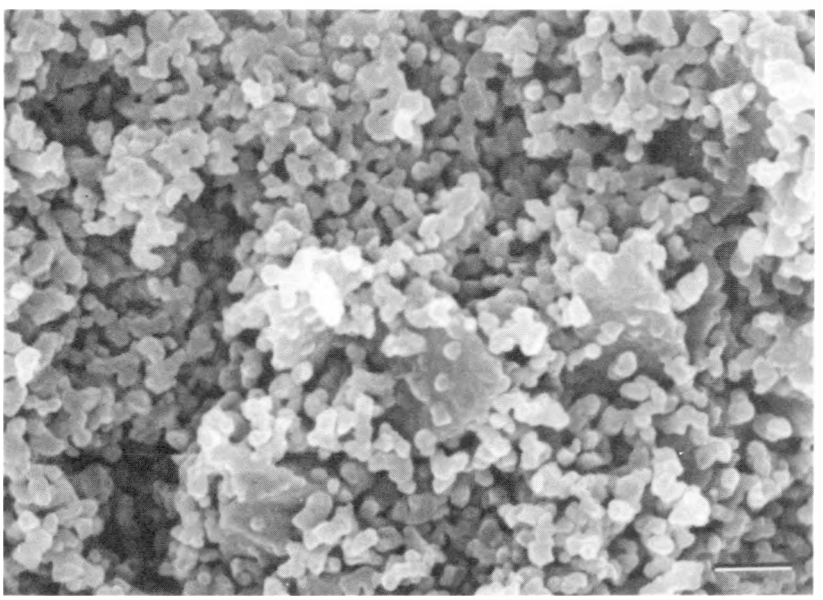

Doped matrix, 20 vol% SiC, sintered to 1100 °C.

Figure 8(e): Bar = 1 μm XBB 911-343

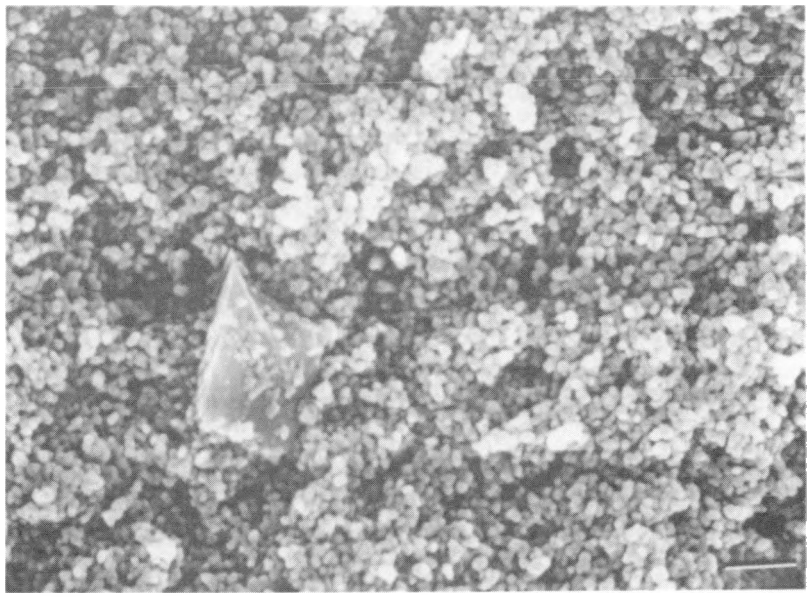

Undoped matrix, 5 vol% SiC, heated to 700 °C.

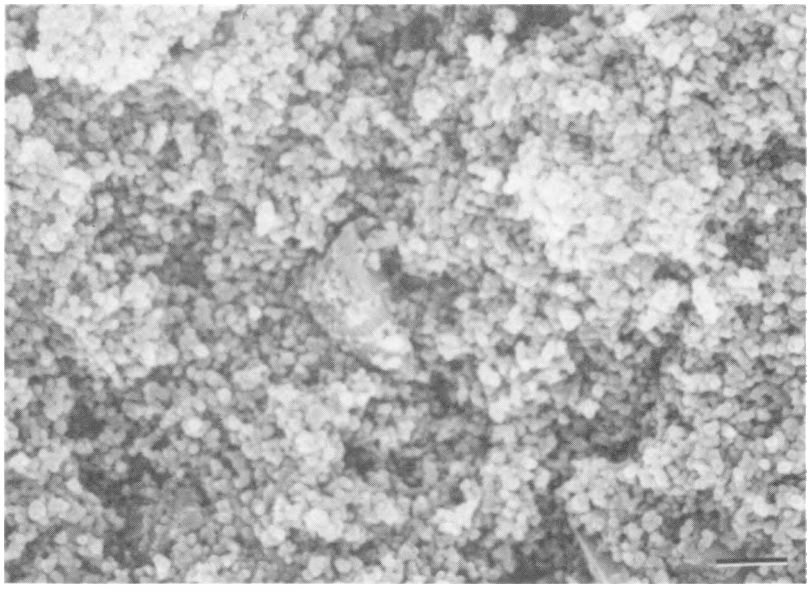

Doped matrix, 5 vol% SiC, heated to 700 °C.

Figure 9(a): Bar = 1 μm. XBB 911-344

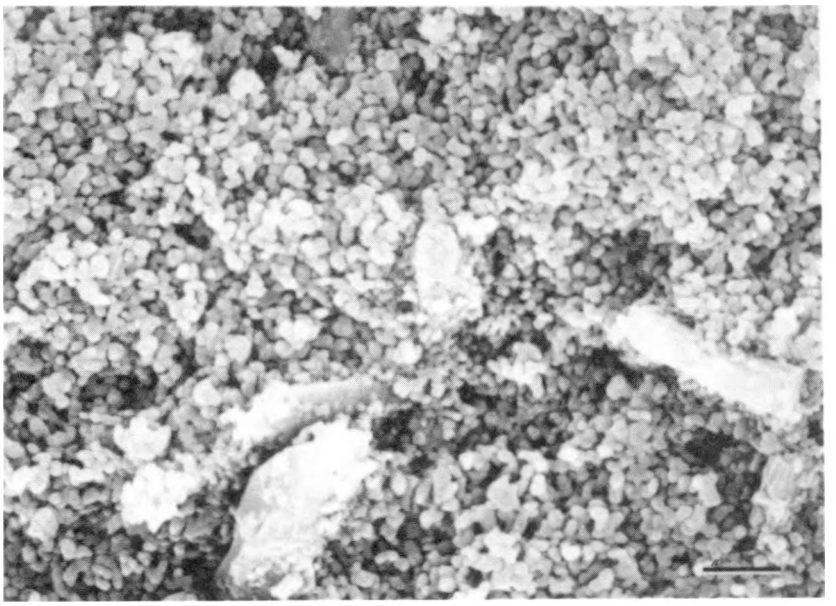

doped matrix, 5 vol% SiC, heated to 800 ^{o}C.

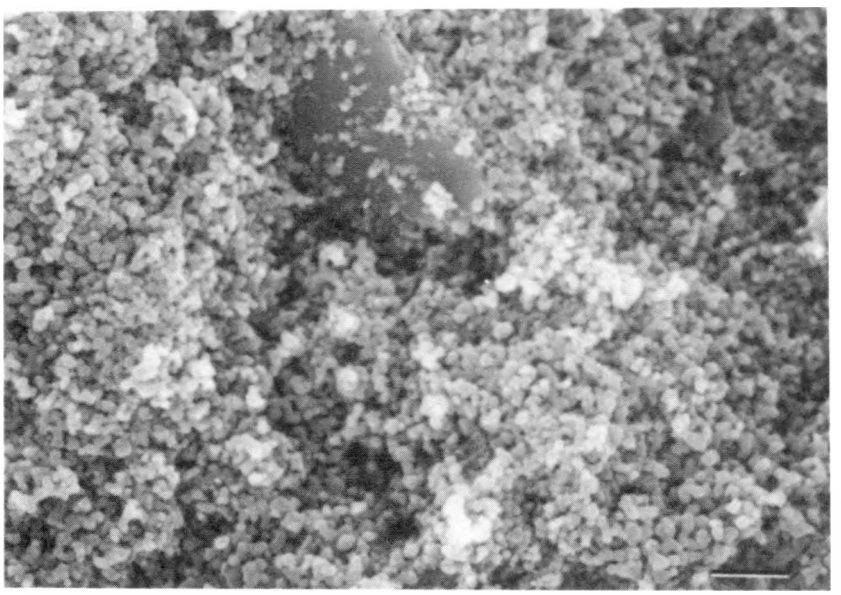

Doped matrix, 5 vol% SiC, heated to 800 ^{o}C.

Figure 9(b): Bar = 1 μm. XBB 911-345

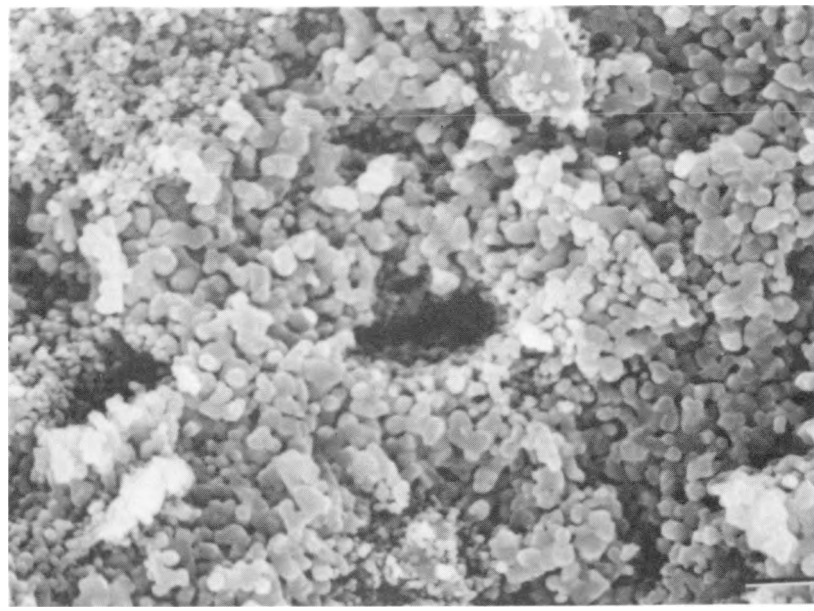

Undoped matrix, 5 vol% SiC, heated to 900 °C.

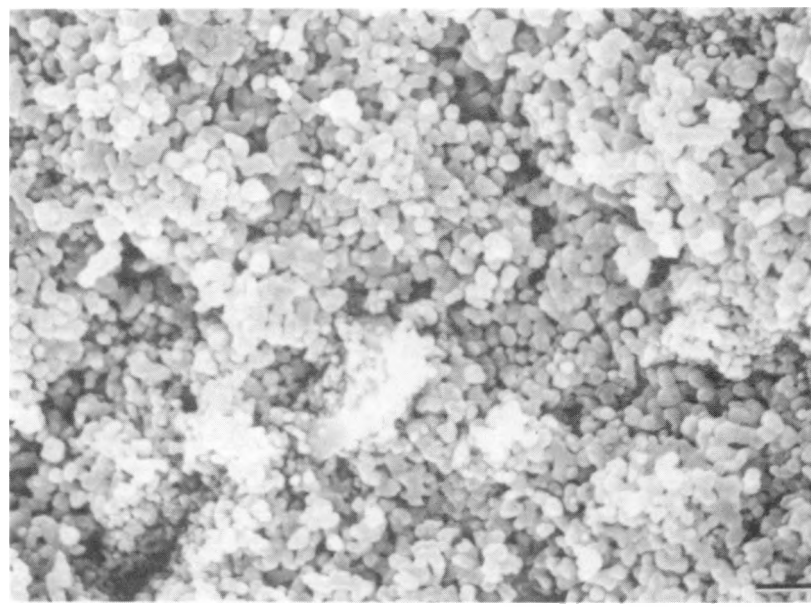

Doped matrix, 5 vol% SiC, heated to 900 °C.

Figure 9(c): Bar = 1μm. XBB 911-346

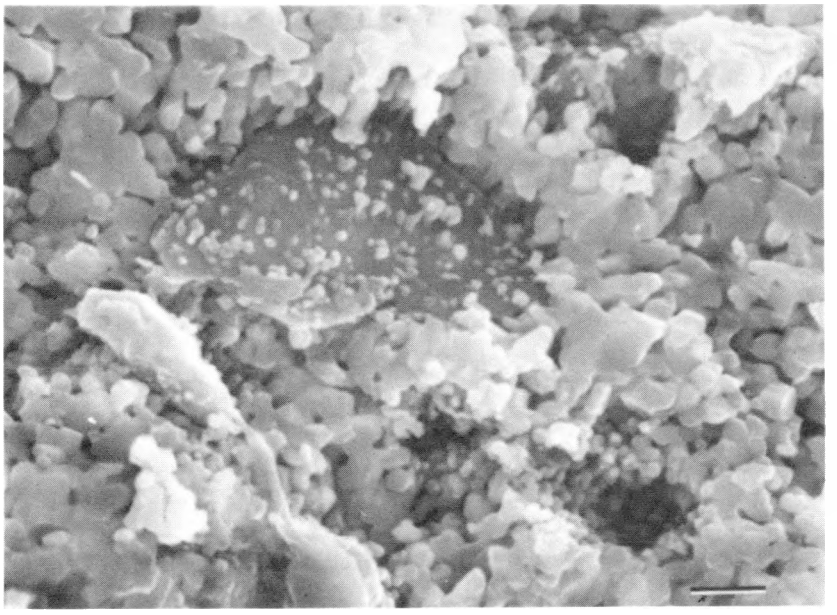

Undoped matrix, 5 vol% SiC, heated to 1000 °C.

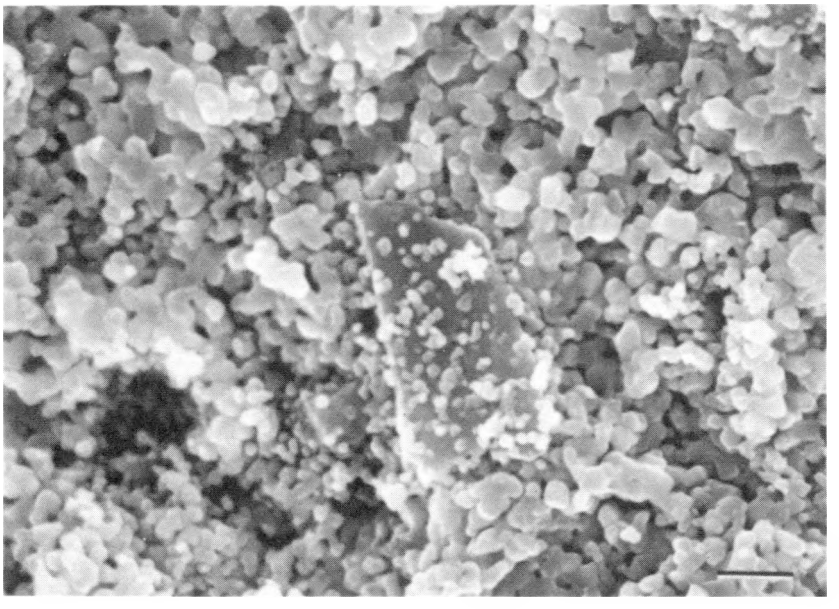

Doped matrix, 5 vol% SiC, heated to 1000 °C.

Figure 9(d): Bar = 1 μm. XBB 911-347

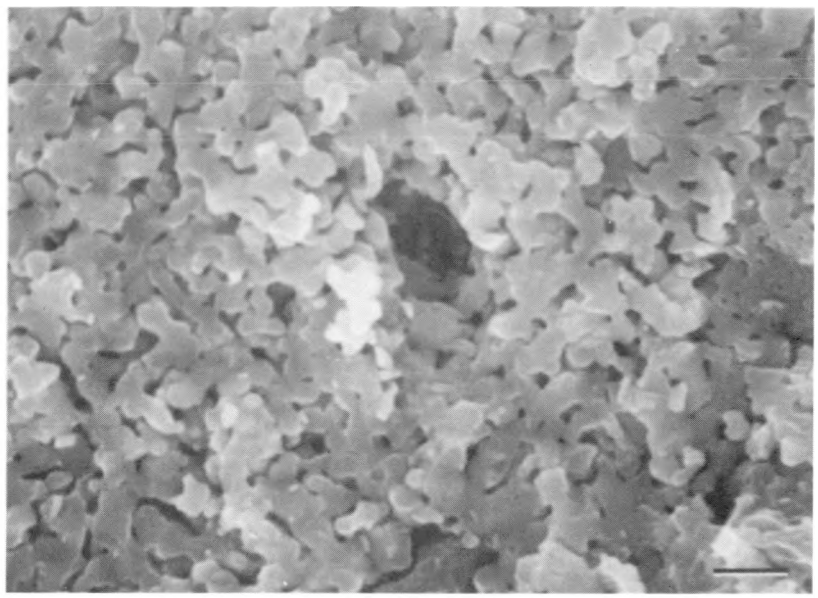

Undoped matrix, 5 vol% SiC, heated to 1100 ^{o}C.

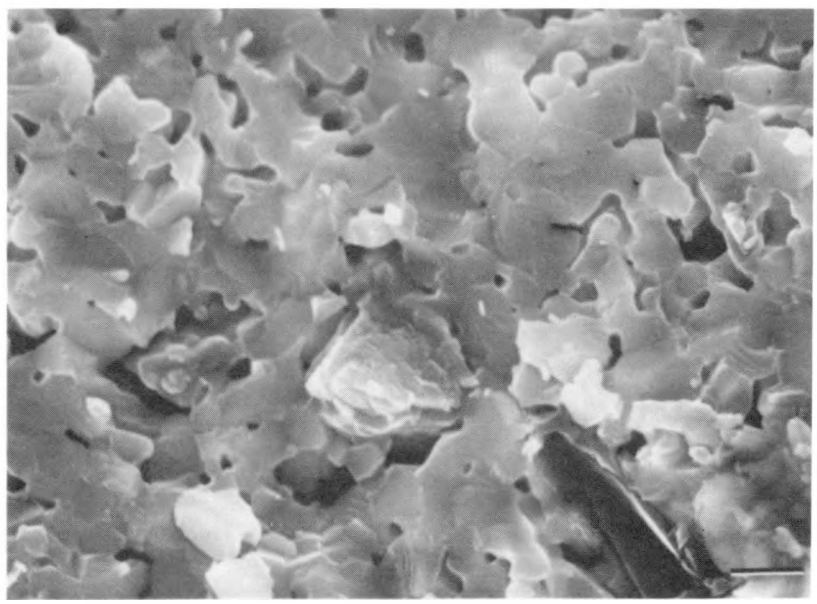

Doped matrix, 5 vol% SiC, heated to 1100 ^{o}C.

Figure 9(e): Bar = 1 μm. XBB 911-349

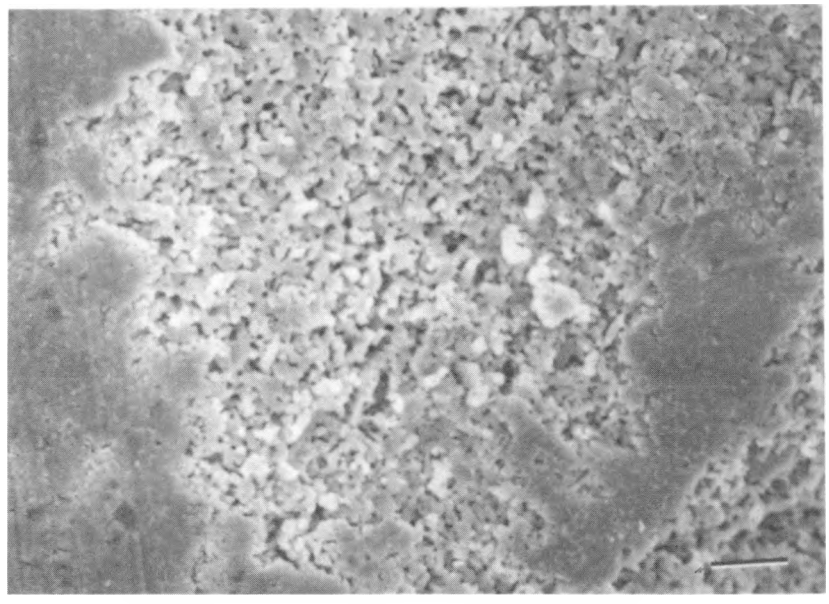

Figure 9(f): Undoped matrix, 5 vol% SiC, showing effects of differential densificat
Bar = 6.62 μm.

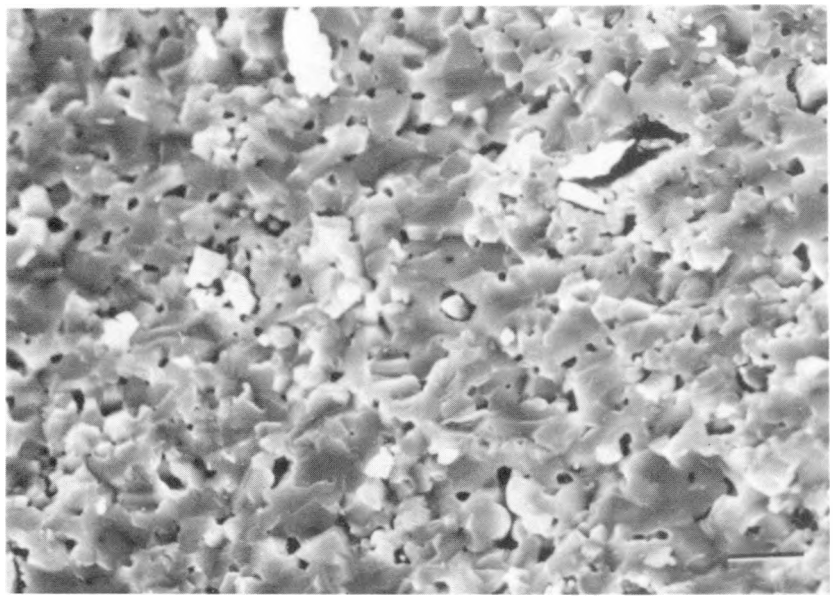

Figure 9(g): Undoped matrix, 1 vol% SiC, showing the formation of voids.
Bar = 3.3 μm.

XBB 911-337

Figure 10: Density vs. Temperature

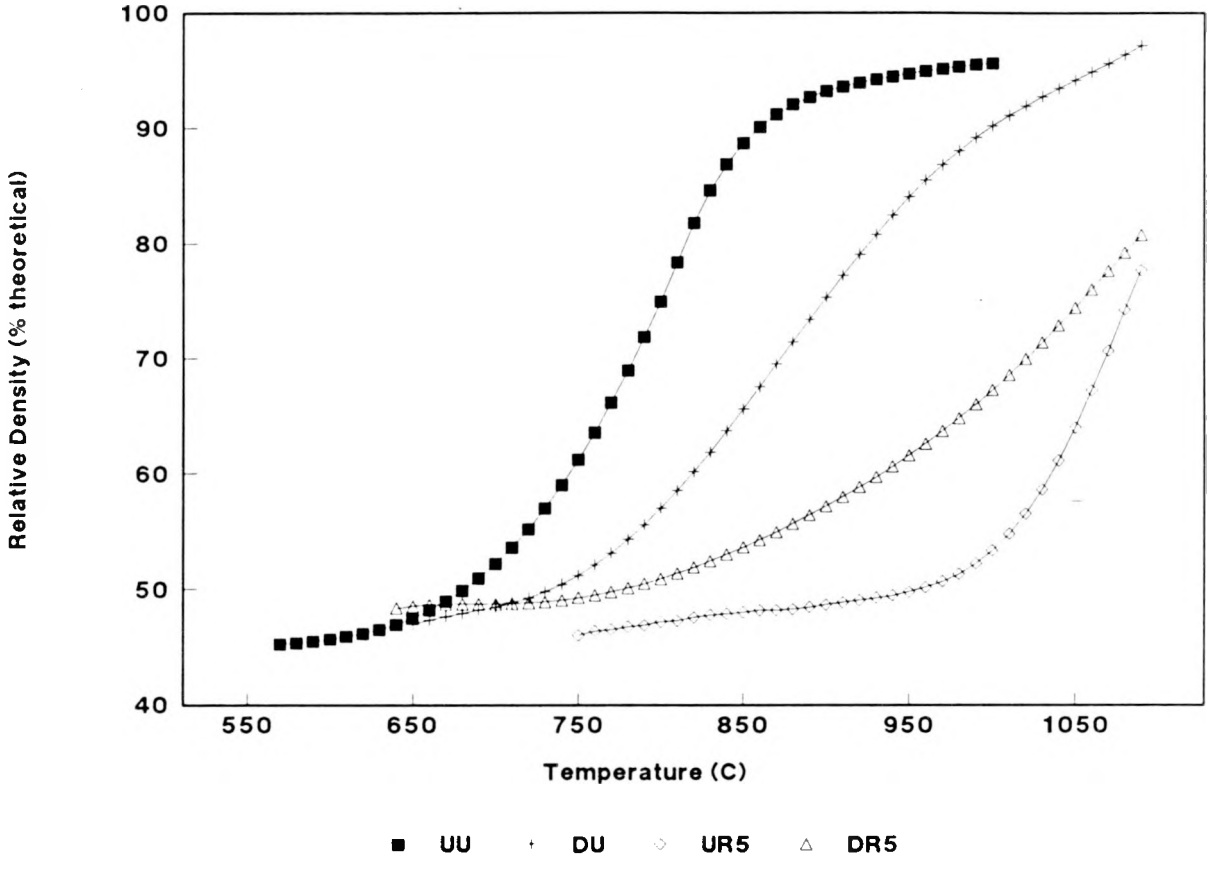

XBL 911-52

Figure 11:Densification Strain vs. Temperature

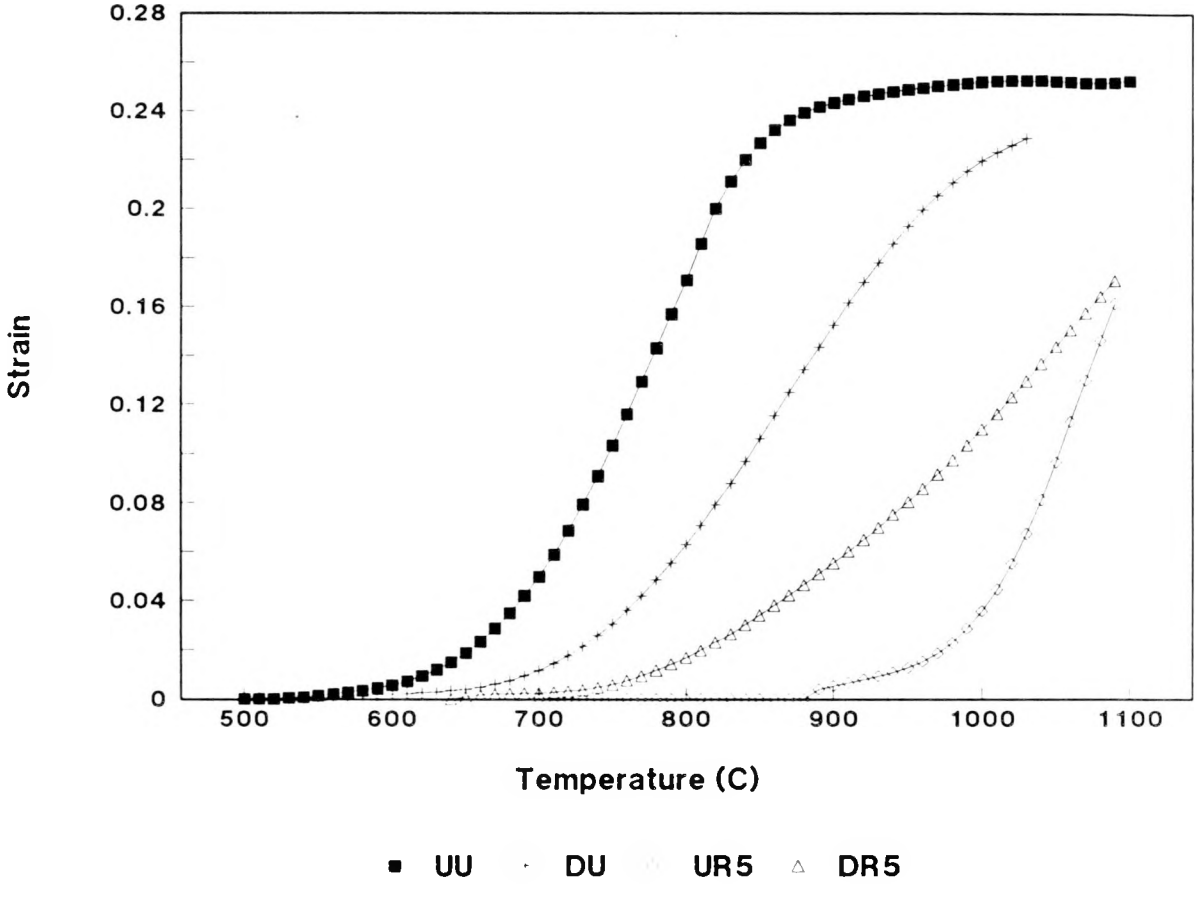

XBL 911-53

Figure 12: Densification Rate vs. Temperature

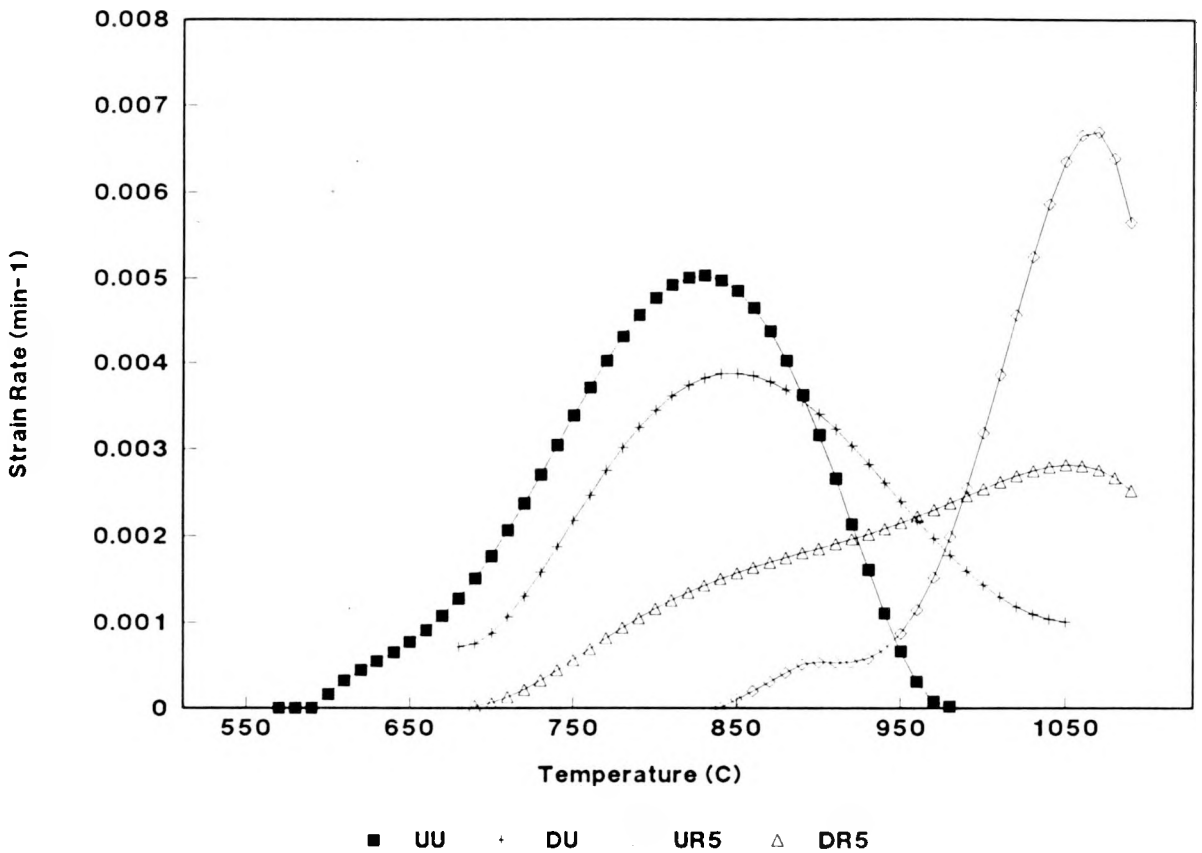

XBL 911-54

Figure 13: Normalized Densification Rate vs. Temperature

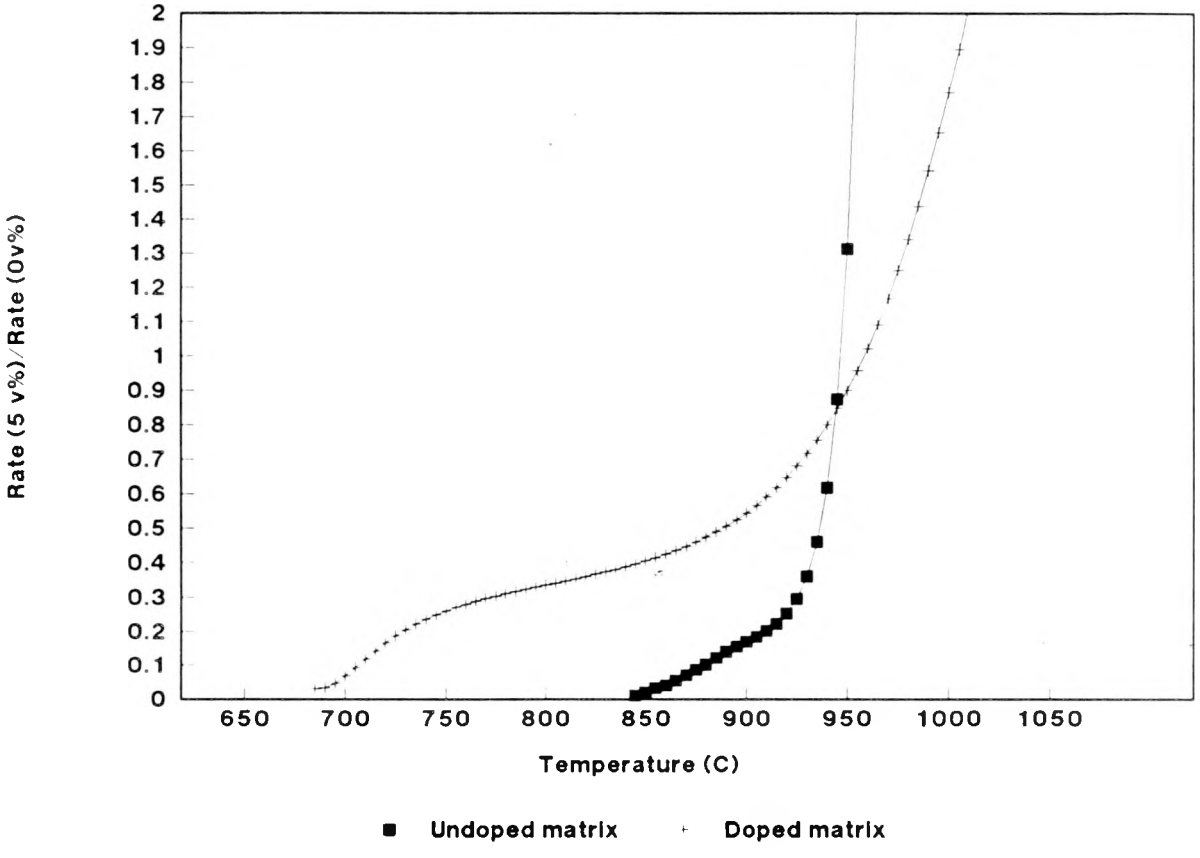

XBL 911-55

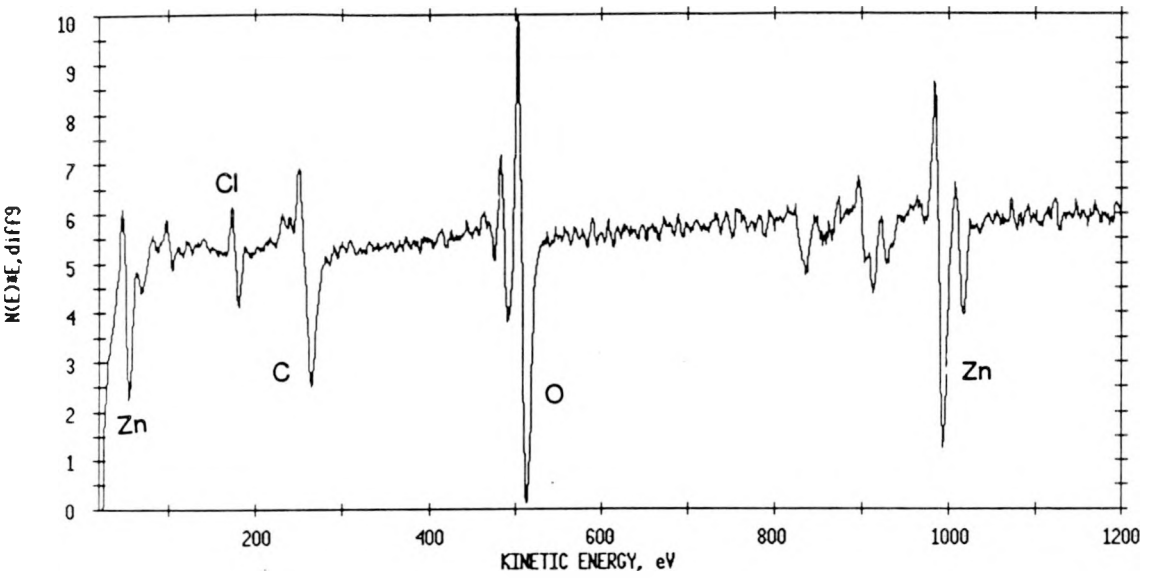

Figure 14: Auger Electron Spectrum of undoped ZnO.

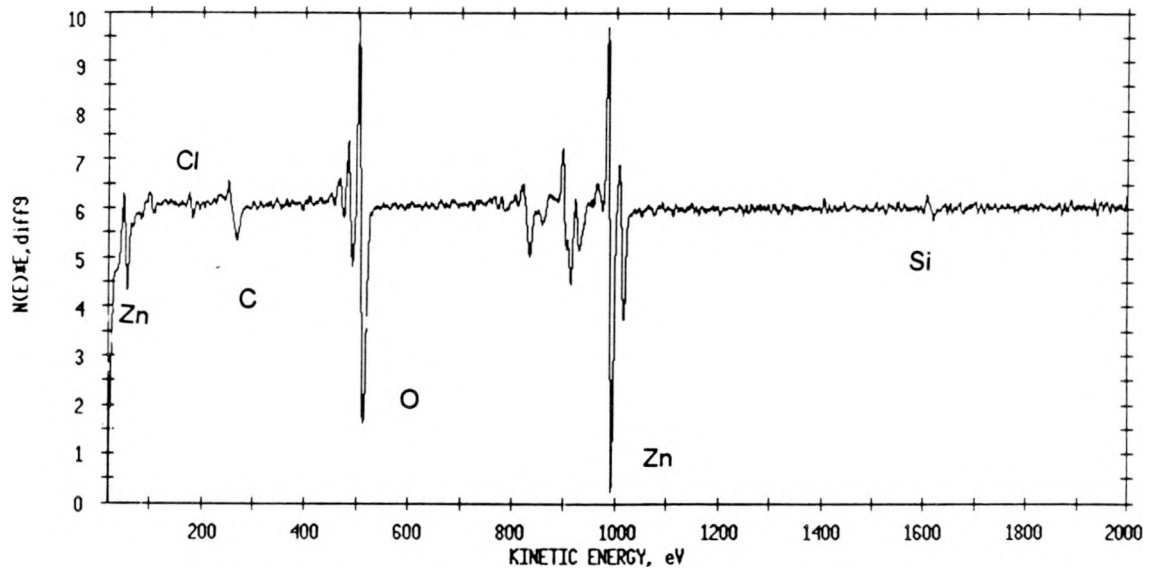

XBL 911-56

Figure 15: Auger Electron Spectrum of undoped ZnO-% vol% SiC composite

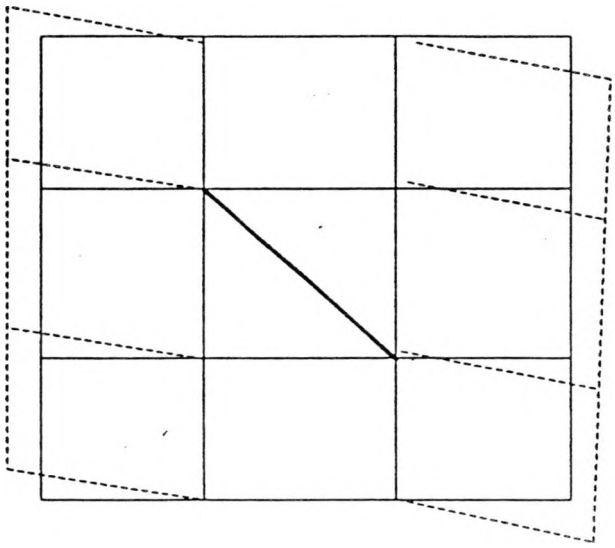

a

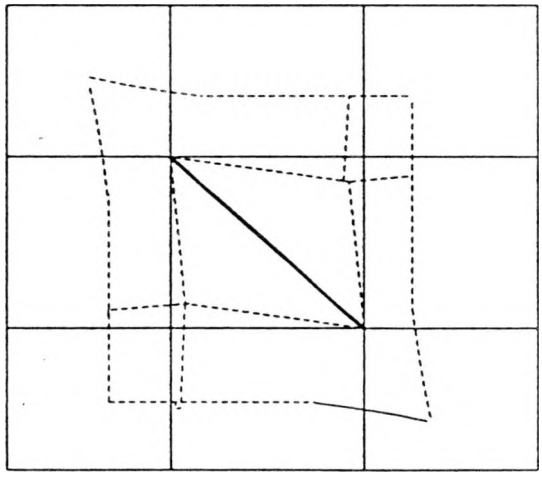

b

Figure 16: Schematic diagram showing the effect of an undeformable inclusion on (a) shear (b) densification.